





## RESEARCH ARTICLE

# Snowmelt and subsurface heterogeneity control tree water sources in a subalpine forest

Stefano Brighenti<sup>1</sup>  | Nikolaus Obojes<sup>2</sup> | Giacomo Bertoldi<sup>2</sup> |  
Giulia Zuecco<sup>3,4</sup>  | Matteo Censini<sup>5</sup> | Giorgio Cassiani<sup>5</sup> | Daniele Penna<sup>6,7</sup>  |  
Francesco Comiti<sup>1,3</sup> 

<sup>1</sup>Faculty of Agricultural, Environmental and Food Sciences, Free University of Bozen/Bolzano, Bolzano, Italy

<sup>2</sup>Institute for Alpine Environment, EURAC research, Bolzano, Italy

<sup>3</sup>Department of Land, Environment, Agriculture and Forestry, University of Padova, Legnaro, Italy

<sup>4</sup>Department of Chemical Sciences, University of Padova, Padova, Italy

<sup>5</sup>Department of Geosciences, University of Padova, Padova, Italy

<sup>6</sup>Department of Agriculture, Food, Environment and Forestry, University of Firenze, Florence, Italy

<sup>7</sup>Forest Engineering Resources and Management Department, Oregon State University, Corvallis, Oregon, USA

## Correspondence

Stefano Brighenti, Faculty of Agricultural, Environmental and Food Sciences, Free University of Bozen/Bolzano, Piazza dell'Università 5, 39100 Bolzano, Italy.  
Email: [stefano.brighenti@unibz.it](mailto:stefano.brighenti@unibz.it)

## Funding information

PRIN MIUR 2017SL7ABC\_005 WATZON

## Abstract

In high mountain areas, snowmelt water is a key—yet fading—hydrological resource, but its importance for soil recharge and tree root water uptake is understudied. In these environments, heterogeneous terrains enhance a highly variable availability of soil and groundwater resources that can be accessed by plants. We conducted a tracer-based study on a subalpine forest in the Italian Alps. We investigated the isotopic composition (<sup>2</sup>H and <sup>18</sup>O) of snowmelt, precipitation, spring water, soil water—at different locations and depths—and xylem water of twigs taken from alpine larch, Swiss stone pine and alpenrose plants during bi-weekly field campaigns (growing seasons of 2020 and 2021). Mixing models based on  $\delta^{18}\text{O}$  revealed a large contribution of snowmelt to soil and xylem water, particularly during early summer. We investigated the contribution of water from different soil depths to xylem water, using the sap flow records to date back the end-member signatures. We found a flexible use of shallow and deeper soil water by the investigated plants, with groundwater more likely used by larger trees and during the late summer. Results based on isotopic data were combined with geophysical observations of the subsurface structure to develop a conceptual model about the different exploitation of water by plants depending on their location (shallow soil on a slope vs. a saturated area). Our study highlights the relevance of snowmelt in high-elevation terrestrial ecosystems, where heterogeneous substrates shape the water availability at different depths and, in turn, water uptake by plants.

## KEYWORDS

coniferous forests, MixSiar, sap flow, snowmelt contribution, stable water isotopes

## 1 | INTRODUCTION

Mountain environments are experiencing drastic climatic changes, with rising temperatures, shifting precipitation patterns and modifications of the duration and timing of winter snow cover (Beniston, 2003; Hock et al., 2019). For example, in the European Alps, snow droughts increased in frequency and magnitude during the last century (Colombo et al., 2023), even though long-term trends in

winter snow are highly variable depending on the area and elevation (Bertoldi et al., 2023). Prolonged growing seasons and warmer summers can cause an increasing demand for tree transpiration, coupled with potential water deficit for plants under dry conditions (Dolezal et al., 2020; Bachofen et al., 2023; Obojes et al., 2018). Thus, understanding how different hydrological sources contribute to soil water recharge and are used by plants is crucial to estimate the potential trajectories of high-elevation ecosystems under a changing climate.

Stable isotopes in the water molecule ( $^{18}\text{O}$  and  $^2\text{H}$ ) are useful tools to investigate the soil–plant–atmosphere interactions within the critical zone (Brooks et al., 2015; Kirchner et al., 2023; Sprenger et al., 2016). These natural tracers are used in field studies to distinguish different water pools within the soil (e.g., Sprenger et al., 2018; 2019), to estimate the contribution of the shallow and deep soil water to tree transpiration (e.g., Barbeta et al., 2019; Dubbert et al., 2019; Penna et al., 2021) or to investigate the rock moisture and its significance for plants (Hahm et al., 2020; Oshun et al., 2016). Ecohydrological isotopic studies are subject to debated uncertainties related to assumptions on natural processes (e.g., Amin et al., 2021; Barbeta et al., 2019; Fabiani et al., 2022), sampling strategies, laboratory analyses and data processing (Beyer & Penna, 2021; Millar et al., 2022). When estimating the root water uptake by plants, an overlooked issue is accounting for travel times between the root water uptake and the moment and location where the tree water is sampled (Giuliani et al., 2023; von Freyberg et al., 2020). This time lag, spanning hours to days and months, is particularly pronounced during the leaf out stage (e.g., Nehemy et al., 2022), and it was addressed as the main driver of the isotopic mismatch between soil and xylem waters in gymnosperms from boreal latitudes (Tetzlaff et al., 2020). However, we are not aware of any attempt to include this travel time lag in mixing modelling analyses.

Some works used stable water isotopes to understand the seasonal origin of soil and plant waters (e.g., Brinkmann et al., 2018). In mountain settings, Zhang et al. (2021) used the seasonal origin index developed by Allen et al. (2019) to demonstrate that larch trees use more winter precipitation than spruce trees in an alpine forest. Similarly, Zhu et al. (2022) highlighted the ecohydrological importance of early summer snowmelt, whose pulse recharges the deep soil layers, and it is then used by *Picea cassiflora* trees. Indeed, in alpine climates, the snowmelt component is known to be a major constituent of water transpired by trees, and it is crucial during the early phenological stages (Nehemy et al., 2022). Despite a progressive mix and dilution with rainfall seeping into the soil, the permanence of a snowmelt component in soil and xylem waters can still be tracked until the end of the growing season (Zhu et al., 2022). While the ecohydrological significance of snowmelt was hitherto investigated in boreal environments (Nehemy et al., 2022), in semi-arid (Zhu et al., 2022) and monsoon influenced (Zhang et al., 2021) mountains of South-Eastern Asia, we are not aware of any similar work carried out in high-elevation, subalpine ecosystems of the European Alps. In such environments, summer precipitation is relatively abundant and evenly distributed in time; hence, a rapid decrease of the snowmelt contribution to xylem water can be hypothesised during the growing season.

Although mountain catchments feature steep slopes with poorly developed soils and rock outcrops, these areas can host abundant groundwater resources (Somers & McKenzie, 2020; Hayashi, 2019). The fractured bedrock beneath the soil can be an important water pool, if trees can access it (Hahm et al., 2020). Furthermore, several mountain landforms host unconfined aquifers where snowmelt/rainfall waters are provisionally stored and from which they are slowly released at springs (Hayashi, 2019; Reato et al., 2022). These

freshwaters may represent potential resources for soil recharge and tree transpiration. Nevertheless, while the literature on the groundwater contribution to tree transpiration is relatively abundant (e.g., Barbeta & Peñuelas, 2017; Engel et al., 2022; Evaristo & McDonnell, 2017; Miguez-Macho & Fan, 2021), the groundwater use by plants is understudied in mountain areas. In a subalpine forest of the Canadian Rocky Mountains, trees showed a peak use of the saturated zone water during early summer, thanks to shallow water table conditions during the snowmelt pulse in a relatively deep soil (Langs et al., 2019). However, the typical substrate heterogeneity of high mountain areas induces a small-scale variability in terms of slope gradient, soil depth and water content and groundwater presence. This variability most likely drives spatially varying water use in trees at different locations (e.g., wetlands influenced by springs or well drained soils). In this framework, geophysical methods can be used as a relatively cheap and non-invasive tool to investigate the subsurface structure on these heterogeneous terrains (e.g., Christensen et al., 2020; Harrington et al., 2018). These methods may support tracer-based findings and aid the development of hydrological conceptual models.

In the present study, we investigated the ecohydrological dynamics of a plot located within a subalpine coniferous forest in the Eastern European Alps (Saldur river basin, South Tyrol, Italy) during two consecutive summers (2020–2021). We aimed to answer the following research questions:

1. What is the contribution of snowmelt and rainfall inputs to soil water at different depths and to xylem water collected from different plants?
2. What is the relative importance of shallow and deep soil water, including groundwater, to plant transpiration while accounting for the xylem water age at the time of sampling?
3. How can geophysical observations improve the conceptualisation of plant water use in the subalpine critical zone?

## 2 | MATERIALS AND METHODS

### 2.1 | Study area

The study area, hereafter referred to as Matscher Alm (Malga Mazia in Italian), is an experimental plot located in South Tyrol/Alto Adige (Eastern Italian Alps), in the upper Saldur catchment. It corresponds to the F5 station of the Long-Term Socio-Ecological Research (LTSER) site Matsch/Mazia (<http://lter.eurac.edu>), established and monitored by EURAC Research (Table 1; Figure 1). Matscher Alm (2050–2090 m a.s.l.) represents a typical subalpine European larch-Swiss stone pine forest on a siliceous substrate (Figure 1b). Geologically, the area belongs to the Ötztal unit (Austroalpine domain), and it is locally composed of banded paragneisses (Autonomous Province of Bozen/Bolzano [APB], 2023). Quaternary deposits are abundant in the catchment underlain by Matscher Alm and include colluvial forms, rock glaciers, moraines and wet meadows. A dense network of streams flows out from these landforms onto a massive, ancient landslide body

**TABLE 1** Meteorological conditions during the growing seasons 2020 and 2021.

	2020	2021
Snowmelt (M4s)	31st of March–12th of April	13th of April/3rd of May
Onset of winter snow	4th of December	27th of November
Growing season—period	6th of May–17th of October	30th of May–24th of October
Growing season—duration	164 days	147 days
Precipitation	501 mm	466 mm
Precipitation/day	3.6 mm	3.2 mm
Air temperature	8.1 ± 4.2 (8.6) °C	8.6 ± 3.5 (8.8) °C

Note: Total precipitation, precipitation/day and air temperature refer to the growing season periods. Air temperature is provided as mean and standard deviation, and median values are in brackets. The growing season and the related number of days refers to the plant LarS (see main text).

(APB, 2023), alternating surface and subsurface reaches. Among these streams, the Matscher Alm borders the north-eastern limits of the plot, which is delimited southward by a slope-hollow-slope morphology. The hollow becomes more evident and incised downslope, with two springs emerging at the lower part of the plot (Figure 1). The upper spring feeds a small wet meadow (of ~30 m<sup>2</sup>) before seeping down into the ground, and it runs dry during late summer. A second spring, where runoff is perennial, is located 25–30 m downstream from the other one, and it represents the outlet of the plot (~4000 m<sup>2</sup>).

The soil (sandy-loam) is shallow (<40–60 cm) and skeletal (rocky clasts  $\Phi = 5\text{--}50$  cm) in the upper part (Obojes, unpublished) and deep (>100 cm) with exclusive presence of fine grains at the wet meadow.

The dominant tree species are European larch (*Larix decidua* Mill.) and Swiss stone pine (*Pinus cembra* L.) that are typical high elevation tree species in the Central Alps, present at different ages and heights. The low density of trees allows the presence of an understory,

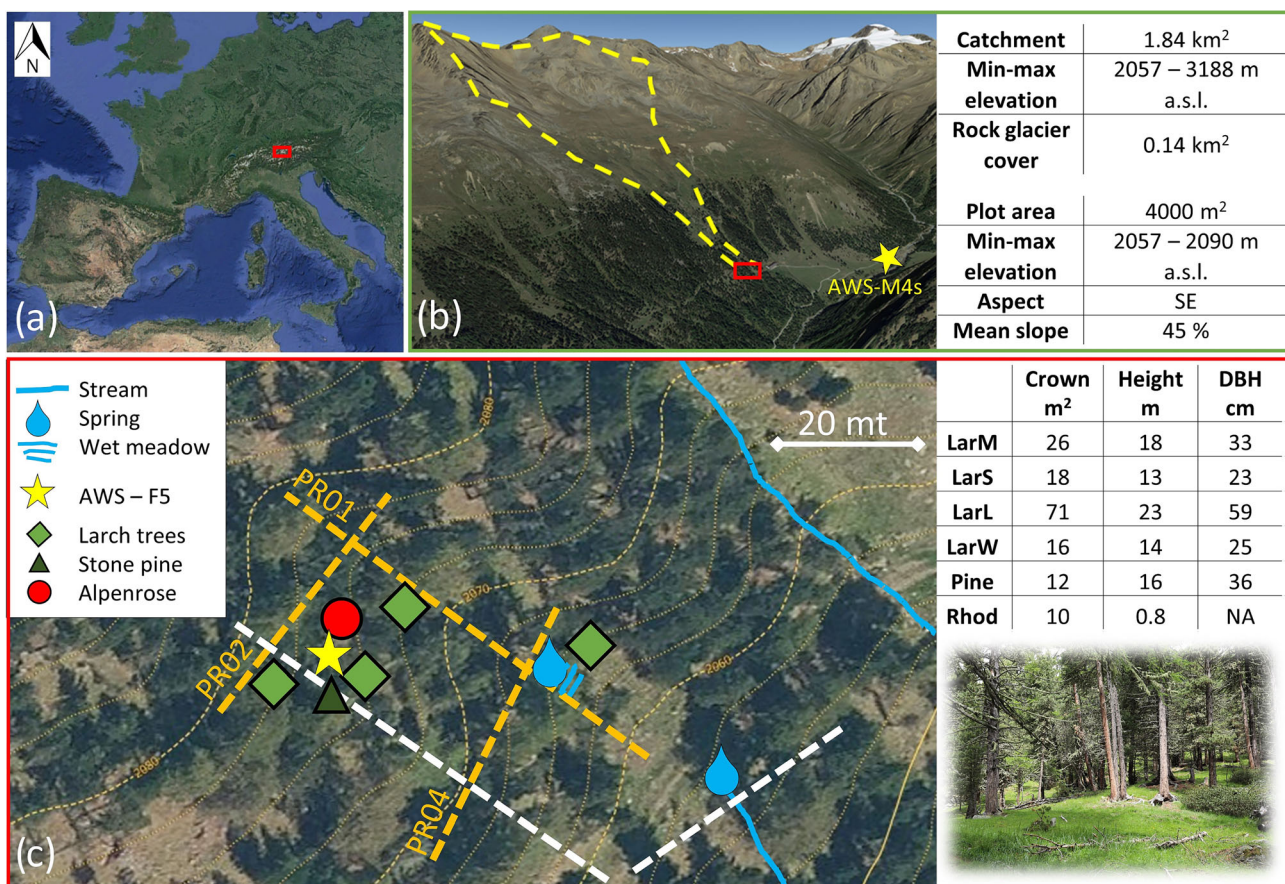


**FIGURE 1** The Matscher Alm plot (a) in the European Alps and (b) within the upper part of the Saldur river basin (Google Earth rendering). The main features of the plot (red frame) and of the Pleres catchment (dashed line) are listed in the right table. (c) Close-up of the plot (aerial images retrieved from Autonomous Province of Bolzano/Bozen [APB], 2022), with highlighted locations of the surface waters and the monitored trees (crown area, height and diameter at breast height—DBH listed in the right table), and a picture of the slope area. Dashed lines indicate the ERT transects (September 2020), and the orange lines indicate the ones that were additionally measured with seismic refraction in June 2021. AWS-F5 and AWS-M4s are the automatic weather stations, managed by Eurac Research.

where dwarf shrubs are mainly represented by sparse alpenroses (*Rhododendron ferrugineum* L.) and european blueberries (*Vaccinium myrtillus* L.).

## 2.2 | Field activities

### 2.2.1 | Sampling campaigns

We conducted bi-weekly field campaigns during the growing season (May–October) of two consecutive years (2020–2021) to collect snow, snowmelt, precipitation, stream and spring waters and soil and twigs samples. Snow and snowmelt water were collected during springtime of both years, before and during the leaf out of larch trees, as solid snow ( $n = 6$ ) and as runoff and water dripping from snow patches ( $n = 10$ ) occurring at Matscher Alm or at adjacent locations.

A rainwater sampler (Palmex Ltd, Zagreb, Croatia) was installed to collect precipitation in an open area of the plot. Two additional HDPE containers, shielded with stones, were installed beneath trees to gather throughfall water. All containers were emptied during each field campaign, after the collection of water aliquots. We also collected the water of the stream and the two springs and measured discharge at the perennial spring by the volumetric method. All water samples were collected in 50 PPE bottles with double cap and filled to the brim.

During each field campaign, we used a soil auger to sample soil at different depths (i.e., shallow: 5–10 cm, 10–15 cm; deep: 25–30 cm, 35–40 cm). During 2020, we collected soil samples in the upper part of the plot, at the hollow and at the slope. During 2021, we also sampled the area of the wet meadow, where the relatively deep soil could be also investigated at an additional depth interval of 70–80 cm. Each sample was collected in three replicates that were placed in 12-mL Exetainer (Labco Ltd, UK) borosilicate containers with pierceable caps. The same containers were used to collect bark-devoid twigs (e.g., Landgraf et al., 2022; two replicates for each tree) from three larch trees of different size (Figure 1) and location at the slope (LarS, LarM) and at the hollow (LarL), respectively. During 2021, we also sampled one larch tree dwelling on the wet meadow (LarW), as well as one alpine stone pine (Pine) and one alpenrose shrub (Rhod) located at the slope.

All samples were placed in thermal bags ( $<6^{\circ}\text{C}$ ) immediately after their collection and taken to the laboratory where they were stored at  $4^{\circ}\text{C}$  until further processing (twigs and soil) and/or analysis (water).

### 2.2.2 | Automatic field monitoring

Data from two automatic weather stations (AWS), a phenocam and sap flow records were made available by Eurac Research (Obojes et al., 2022). Data on snow height (cm) were retrieved from the AWS-M4s (2015 m a.s.l., operative from 2020), located close to the plot (Figure 1b). Time series of air temperature ( $^{\circ}\text{C}$ ), precipitation (mm) and soil water content ( $\text{m}^3 \text{m}^{-3}$ ) at different depths (Campbell CS655

probes at 5, 20 and 50 cm) were retrieved from the AWS-F5 (2080 m a.s.l., operative from 2015), located within the plot (Figure 1c). To increase the data on soil water content, we installed six soil probes (TMS-4; Tomst Ltd., Czech Republic) recording electromagnetic time domain transmissions at 15-min resolution. These sensors were installed during June 2020 at different depths (10 cm, 20 cm, 35 cm) in the upper part of the plot, at the hollow and at the slope. We converted the electromagnetic data obtained with TMS-4 probes in volumetric water content values using the TMS Calibr Utility and applied soil conversion factors based on the soil density and granulometric composition at different layers.

We also retrieved the data of sap flow records, measured with tissue heat balance sensors (Cermak et al., 2004) EMS51 (EMS, Brno, Czech Republic) located at breast height (1.3 m) at Pine, LarL, LarM and LarS trees and managed by Eurac Research. These sensors measure the heat input power required to keep a one degree Kelvin difference between three heated electrodes and an unheated electrode installed 10 cm below, which is directly correlated to sap flow. Initial sap flow density provided in  $\text{kg h}^{-1} \text{cm}^{-1}$  of circumference unit was converted into sap flow volumes (in  $\text{L h}^{-1}$ ) per tree by multiplying them with the respective stem circumference (minus bark and phloem thickness) according to Kučera (2010). Time series (10- to 15-min records, depending on the parameter and sensor) were rescaled to consistent hourly and daily intervals.

Daily images (hourly pictures from 9 AM to 5 PM) from a phenocam (Plotwatcher Pro game camera; Columbus, GA, USA) focused on the branches of one of the monitored larch trees (LarL) were investigated to distinguish different moments of the growing season (simplified from Migliavacca et al., 2008): leaf out (i.e., visible budburst–maximum expansion of the needles), main growing season and the decolouration phase (i.e., yellow spot decolouration–complete bronze crown/needles lost).

### 2.2.3 | Geophysical investigations

To investigate the subsurface structure of the ground, we performed electrical resistivity tomography (ERT) and seismic refraction (SR) transects. The first technique was used to investigate the electrical properties of the ground based on the propagation of electric current in the ground and measuring the electrical potential at various points along a section. We used Dipole–Dipole multielectrode profiles with Syscal Pro Switch-48 (Iris Instrument, Orléans, France) georesistivity meter. Data acquisition was performed by placing the electrodes at one-metre steps, in two longitudinal profiles (along the hollow and the slope) and two cross-section (upslope and downslope) transects (Figure 1c). Acquired data were processed with the dedicated softwares Prosys II (Iris Instrument) and RESIPY (Blanchy et al., 2020). SR was used to investigate the elastic properties of the ground based on the compression wave velocities. This makes it possible to estimate the mechanical and physical properties of soils and the compactness of the materials that seismic waves pass through. SR was performed along the hollow and two transverse transects used for ERT analyses,

and geophones were placed into the ground every 2 m. Seismic signals were acquired with a 24ch DAQLink 3 with 24-bit resolution from Seismic Source Co. All results are displayed in S1.

## 2.3 | Laboratory activities

At the Faculty of Science and Technology of the Free University of Bozen/Bolzano (Italy), we used the cryogenic vacuum distillation technique (Koeniger et al., 2011) to extract the water from the soil and the twigs (xylem water) samples. We used the same instruments, procedure, heating temperature (200°C) and extraction times (15 min) described in Zuecco et al. (2022). Exetainer vials were weighted before and after the cryogenic distillation, and after oven treatment (48 h, 105°C), to estimate the extraction efficiency ( $R_{\text{eff}}$ ). We only analysed water samples associated with  $R_{\text{eff}} > 98\%$ , and cryogenic distillation was repeated on sample replicates if this minimum efficiency was not achieved. Overall,  $R_{\text{eff}}$  for the analysed samples was 99.3 (median 99.6)  $\pm$  0.6% (standard deviation) for twigs and 99.7 (99.8)  $\pm$  0.9% for soils.

The isotopic composition ( $\delta^2\text{H}$ ,  $\delta^{18}\text{O}$ ) of snowmelt, precipitation, stream and spring waters was determined with a laser spectrometer (CRDS Picarro L2130i, CA, USA). The precision of the analyser was 0.5‰ for  $\delta^2\text{H}$  and 0.25‰ for  $\delta^{18}\text{O}$ . The memory effect (Cui et al., 2017) was minimised following the procedure reported in Penna et al. (2012). Xylem and soil waters were analysed with isotope-ratio mass spectrometry (IRMS Delta V Advantage Conflo IV, Thermo Fisher Scientific Inc., Waltham, Massachusetts, USA), with a precision of 2.5‰ for  $\delta^2\text{H}$  and 0.25‰ for  $\delta^{18}\text{O}$ . All isotopic results were referred to the Vienna Standard Mean Oceanic Water and expressed in ‰ notation. The correlation of the isotopic values obtained with the IRMS and the CRDS on 19 samples (internal standards and throughfall water samples) showed a mean absolute error of 0.50‰ for  $\delta^2\text{H}$  and 0.06‰ for  $\delta^{18}\text{O}$ .

## 2.4 | Analysis of isotopic data

The isotopic deviation of the samples from the local meteoric water line (LMWL, Rozanski et al., 1993) was calculated as corrected line conditioned excess (Lc-excess\*; Landwehr & Coplen, 2006). Lc-excess\* was computed as follows:

$$Lc - excess^* = \frac{\delta^2\text{H} - a \times \delta^{18}\text{O} - b}{S} \quad (1)$$

where  $a$  and  $b$  are the slope and the intercept of the LMWL and  $S$  was determined as follows:

$$S = \sqrt{SD_{\delta^2\text{H}}^2 + (a \times SD_{\delta^{18}\text{O}})^2} \quad (2)$$

SD are the typical instrumental standard deviation of both isotopes (2.5‰ and 0.10‰ for  $\delta^2\text{H}$  and  $\delta^{18}\text{O}$ , respectively; see also

Zuecco et al., 2022). We analysed differences in isotopic composition between groups based on nonparametric pairwise comparisons with the Wilcoxon signed rank test (SPSS Statistics software, v.27; IBM, 2018).

### 2.4.1 | Snowmelt/rainfall contribution to freshwaters, soil and xylem water

Based on  $\delta^{18}\text{O}$  measurements (less prone to fractionation than  $\delta^2\text{H}$ ), we used end-member mixing models to estimate the contribution from snowmelt and rainfall to spring water, soil water at different locations and depths and xylem water in different trees. We used the package MixSIAR v. 3.1.12 (Stock et al., 2018; Stock & Semmens, 2016) in R v. 4.1.2 (R Core Team, 2021). The end-members estimation and the MixSIAR specifications are described more in detail in Data S2. To estimate the drivers of the seasonality in the snowmelt component, we calculated the day of the year (DOY, i.e., days elapsed from the New Year's Day), day after snowmelt (DAS, i.e., the day elapsed from the complete vanishment of the snow cover at the AWS - M4s) and day after leaf out (DAL, i.e., the day elapsed from the onset of leaf out as spotted with the phenocam). Then, we followed the procedure outlined by Stock et al. (2018) to choose the best indicator of the seasonality in the snowmelt/rainfall components (Data S2). To estimate the seasonality in the snowmelt contribution (response variable) at different water compartments, we used the best candidate among DAS, DOY and DAL continuous covariates, as a smooth term in generalised additive models (GAMs), with AR1 autocorrelation. We applied GAM beta regression with logit link function (*betar* family in R *mgcv* package; Wood, 2023) on 0–1 normalised data.

### 2.4.2 | Contribution from different subsurface depths to xylem water fluxes

Based on the soil water signatures ( $\delta^{18}\text{O}$ ) of the location where each tree was located (hollow, slope, wet meadow), we calculated the contribution of shallow and deep soil water to xylem water in time-variant (i.e., end-member signatures varying over time), linear end-member mixing models. When the xylem water was isotopically more depleted than the deep soil water, we considered as end-members the groundwater resources and the bulk soil water (detailed methodology in Data S2). We applied three distinct scenarios to define the end-members for each xylem water sample. Under a 'synchronic' scenario, we used the soil isotopic values of the same day when the twig samples were collected. Under a 'delayed' scenario, we used the values of soil waters and groundwater belonging to the samples collected during the previous sampling campaign (10–18 days earlier). We assumed the signature of each soil depth as a linear combination between those of the same sampling day and those of the previous (linear regression) or previous two (polynomial function,  $n = 2$ ) samplings (depending on the modelled age of the xylem water). Under a 'xylem water age' scenario, we used the sap flux records to date back

the isotopic signature of each end-member during the simulated (tree- and date-specific) day of root water uptake from the ground. This scenario could be applied only to the trees where we monitored sap flow. For each tree, we converted the sap flow volumes ( $L h^{-1}$ ) into sap velocities ( $mm h^{-1}$ ) considering the measured diameter as well as the bark and the sapwood depths at breast height. Then, for each tree

and moment of sampling, we back calculated the time (h) that was necessary for the xylem water to reach the sampled twig, using the velocity records of the period antecedent the sampling (detailed methodology in Data S3).

We accounted for gaussian error propagation (Genereux, 1998) to estimate the uncertainties of the mixing model outcomes. The

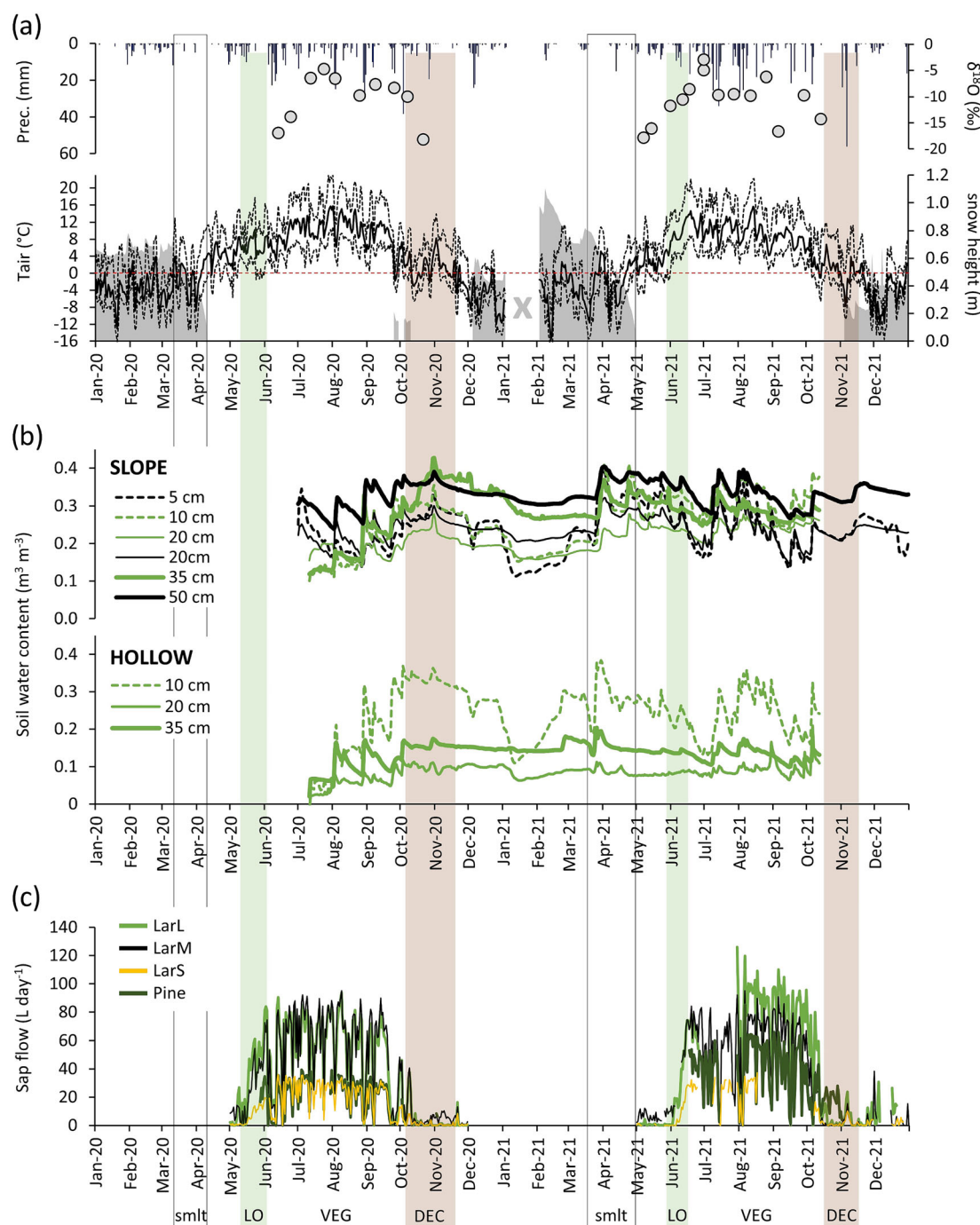


**FIGURE 2** Climatic and phenological conditions of the Matscher Alm during the years 2020/2021. (a) Series of daily precipitation and  $\delta^{18}O$  values of integrated precipitation (dots), air temperature and snow cover height. The 'X' symbol represents periods of missing data; (b) volumetric soil water content data at different depths in the hollow and slope soils. Series from different sensor types are coloured differently (green = TMS-4; black = Campbell); (c) daily sum of sap flow of the monitored trees. Smilt = snowmelt period; LO = leaf out, VEG = main growing season, DEC = decolouration phase.

uncertainties of the xylem water age scenario are provided as mean of the ones from the other two scenarios.

### 3 | RESULTS

#### 3.1 | Meteorological series and tree phenology

Similar air temperatures and cumulative precipitation occurred in 2020 and 2021 (Table 1). Most precipitation (66% during 2020 and 63% during 2021) fell during the growing period (Table 1). The snow cover period was 21 days longer in 2021 than in 2020. The period of major tree transpiration started earlier during 2020 (24 days), even though the 2 years had a comparable duration in terms of growing period. Soil water content sensors revealed seasonal patterns related to snowmelt wetting in spring and snow cover onset in winter (Figure 2b), when soil water decreases due lack of liquid water input. The winter soil water decrease in the surface layers is due soil freezing. During the growing period, soil water recharge occurred when snowmelt faded out throughout the soil column, and only rainfall events transiently rewetted it.

Daily sums of sap flow were highly variable depending on solar radiation and air vapour pressure deficit and did not reveal any

evidence of water deficit in the monitored plants during the growing season (Figure 2c). In this period, sap velocities were about  $1 \text{ m day}^{-1}$ , with LarM ( $1.5 \pm 0.8 \text{ m} \cdot \text{day}^{-1}$ ) having higher fluxes than LarS ( $1.1 \pm 0.6 \text{ m} \cdot \text{day}^{-1}$ ), LarL ( $0.7 \pm 0.4 \text{ m} \cdot \text{day}^{-1}$ ) and Pine ( $0.3 \pm 0.3 \text{ m} \cdot \text{day}^{-1}$ ). Thus, assuming the sampling position at single trees, during the main growing season, xylem water roughly required 1–5 days to cross the trunk and reach the sampled twigs, with lower transit times for LarS, Pine and LarM. In contrast, during the leaf out period, all velocities were very low (in the order of  $\text{cm day}^{-1}$ ) so that the age of the xylem water in the sampled twigs was in the order of 150–250 calendar days, that is, corresponding to the previous autumn (Data S3).

#### 3.2 | Spatial variability of the subsurface structure

Seismic and electric surveys revealed a pronounced spatial heterogeneity of the subsurface morphology (Figure 3). ERT lines showed contrasting resistivities based on location and depth. In the upper part and the south-western lower part of Matscher Alm, where most of the investigated plants were located, resistivity values were generally high ( $>3000 \Omega \text{ m}$ ) at all depths (i.e., down to 12 m below the ground). Within the hollow, a ramp of lower resistivity values ( $500\text{--}1000 \Omega \text{ m}$ )

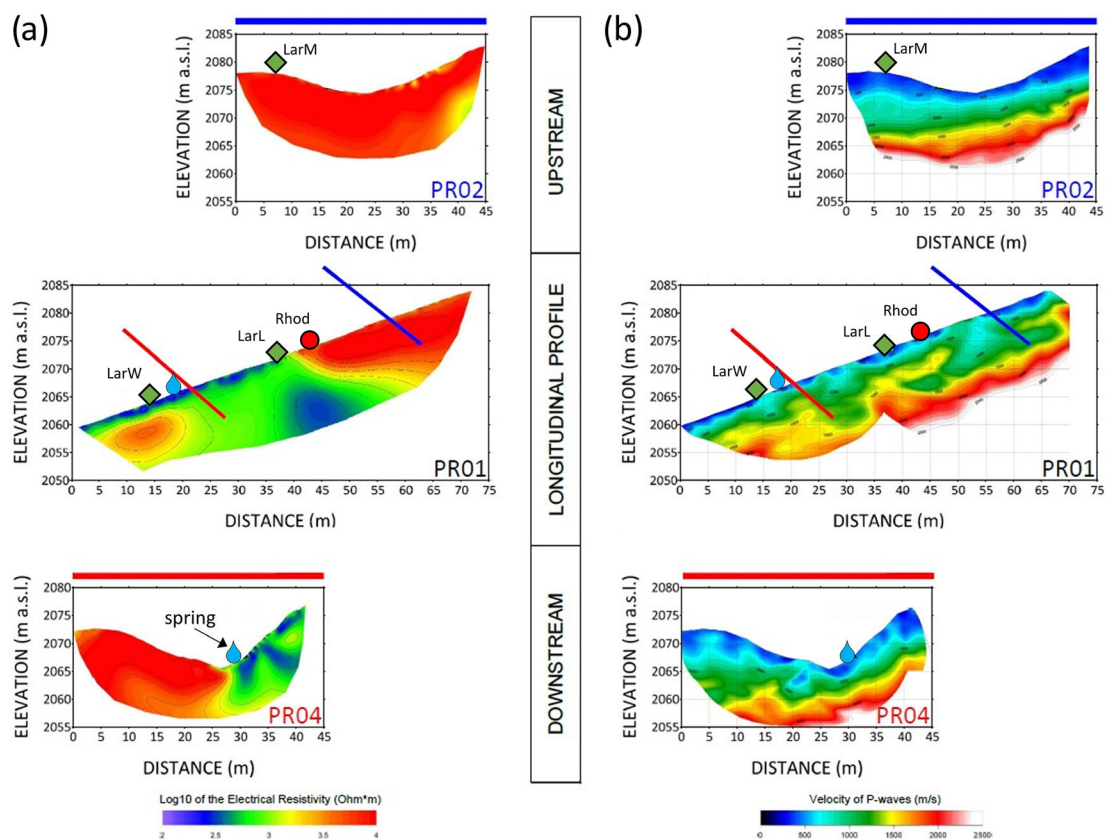


**FIGURE 3** Results of the geophysical investigations conducted for the upstream, longitudinal and downstream transects. For each transect (see Figure 1), the bidimensional representation of electrical resistivity (a) and propagation velocities of seismic waves (b) are displayed. As reference, the intersections of the upstream (blue) and downstream (red) transect with the longitudinal profile are provided (PR01). The drop symbol represents the location of the spring at the wet meadow.

was gradually more surficial when moving downslope. At the springs and the wet meadow, the shallow ground (<5-m depth) had resistivity values in the order of 500–600  $\Omega$  m (Figure 3a). The results from SR confirmed the large subsurface heterogeneity along the hollow, with low wave velocities (500–1000  $\text{m s}^{-1}$ ) in the shallow ground (<5-m depth), increasing with depth (up to 2000–2500  $\text{m s}^{-1}$  at 10- to 12-m

depth). Rather than a uniform gradient of increasing velocities with depth, the propagation of waves was organised in pockets of low velocities located in tables of higher velocities, bringing a disorganised conformation of the seismic wave propagation (Figure 3b). Overall, these analyses revealed a surface structure of a typical landslide body, with fine-scale heterogeneity of loose and compact materials related

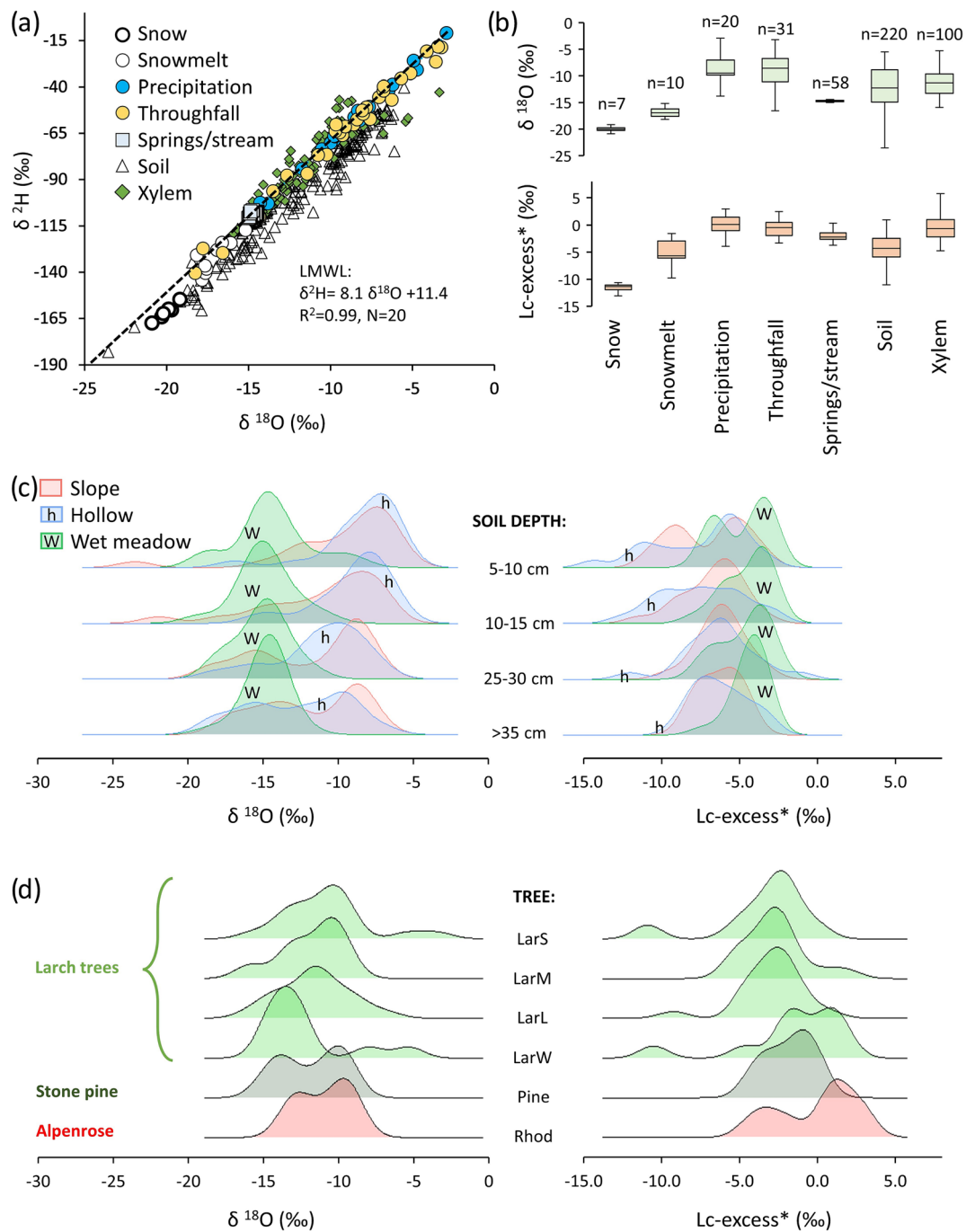


**FIGURE 4** Isotopic overview of the waters analysed at the Matscher Alm. (a) Dual isotope plot of the main water types. The LMWL of the Matscher Alm and its equation is very similar to that described by Penna et al. (2014; as  $\delta^2\text{H} = 8.1 \delta^{18}\text{O} + 10.3$ ) for the Saldur river basin; (b) boxplots of  $\delta^{18}\text{O}$  and Lc-excess\* categorised based on the main water types. (c) Ridgeline plots for  $\delta^{18}\text{O}$  and Lc-excess\* at different soil depth classes (y-axis, in common), showing data distributions at different locations (slope, hollow and wet meadow). (d) Same type of ridgeline plots, with the different sampled plants at the y-axis. Note: to allow graphical comparisons of soil and xylem waters, the scales of (c) and (d) are identical and placed in line.



to the organisation of boulders and finer materials. Below the first couple of metres made of loose materials, the ground was progressively more compacted, and the depth of the non-fractured bedrock was assumed at 7–15 m, depending on the location in the hollow (Figure 3b). Moreover, geophysical data revealed well the softer or more wet soil in the hollow that is related to the spring (Figure 3a).

### 3.3 | Isotopic composition of the different water pools

Different types of water had distinct isotopic composition (Figure 4). Values of precipitation aligned on the dual isotope plot, shaping an LMWL (Figure 4a) that almost overlapped with that described by

Penna et al. (2014) derived for the Saldur River basin. The intercept and the slope of the LMWL were typical of an alpine climate (Putman et al., 2019) with a major influence from Atlantic air masses (Penna et al., 2014). The isotopic signature of precipitation had a unimodal behaviour typical of the alpine seasonality, with more negative values during May/June (interquartile range—IQR of  $\delta^{18}\text{O} = -16.1/-10.5\text{‰}$ ) and September/October (IQR  $\delta^{18}\text{O} = -15.5/-9.0\text{‰}$ ) enhanced by low air temperatures bringing rain/snow or snow events during these periods (Figure 2a). The isotopic fingerprint of throughfall was not significantly different to that of precipitation (Figure 4b). Snowmelt samples had significantly lower ( $p < 0.001$ ) isotopic values and Lc-excess\* when compared with precipitation and throughfall (Figure 4b). The stream and the two springs showed overlapping isotopic signatures and little variability over time. The isotopic signature

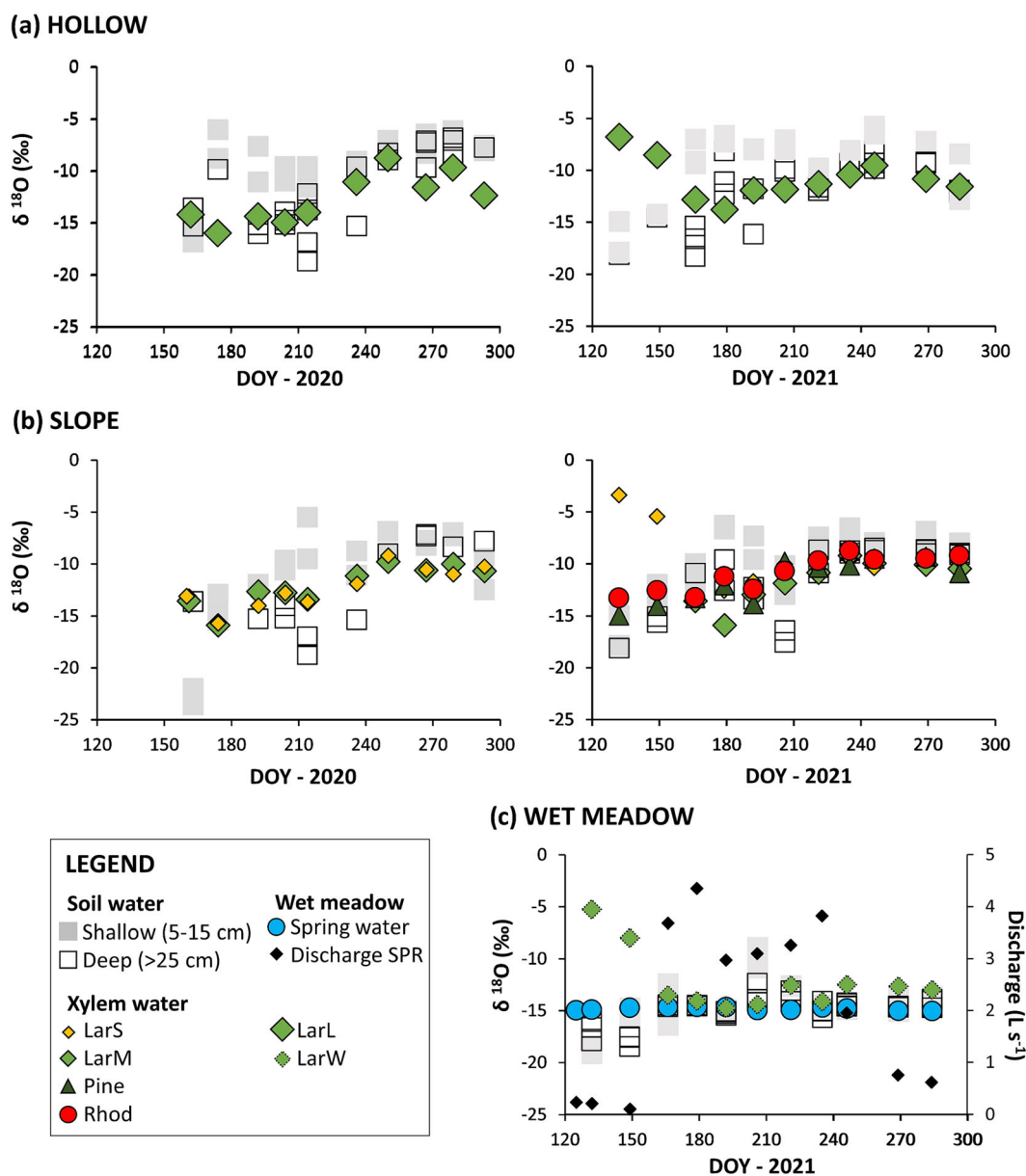


**FIGURE 5** Values of  $\delta^{18}\text{O}$  over time (day of the year—DOY) in the soil and xylem waters, at (a) the slope, (b) the hollow and (c) at the wet meadow. In the latter, we also provide isotopic values and discharge at the lower spring.

of the bulk soil water had a large spatial (Figure 4c) and temporal (Figure 5) variability. At the slope and at the hollow,  $\delta^{18}\text{O}$  had a seasonal asymptotic behaviour, a progressive isotopic enrichment from May to July, and relatively steady values when moving towards October. This was more evident at lower depths. In fact, there was a tendency of decreasing isotopic values and increasing Lc-excess\* towards greater soil depths (Figure 4c), even if this was not true for all sampling dates and locations (Figure 5). At the wet meadow, both the xylem water and the soil water were generally more depleted in heavy

isotopes, and there was a tendency of increasing isotopic values with depth and of isotopic overlapping between the deep soil and the upstream spring isotopic values (Figure 4c).

Xylem water had a similar isotopic composition as soil water (Figure 5c) and a comparable seasonal trend except during the period of leaf out (Figure 5a-c). In fact, during this time, the investigated larch trees had the highest isotopic enrichment on a seasonal basis and in agreement with xylem samples from twigs collected during wintertime ( $\delta^{18}\text{O} = -6.7/-8.4\%$ , not displayed), when no sap flow

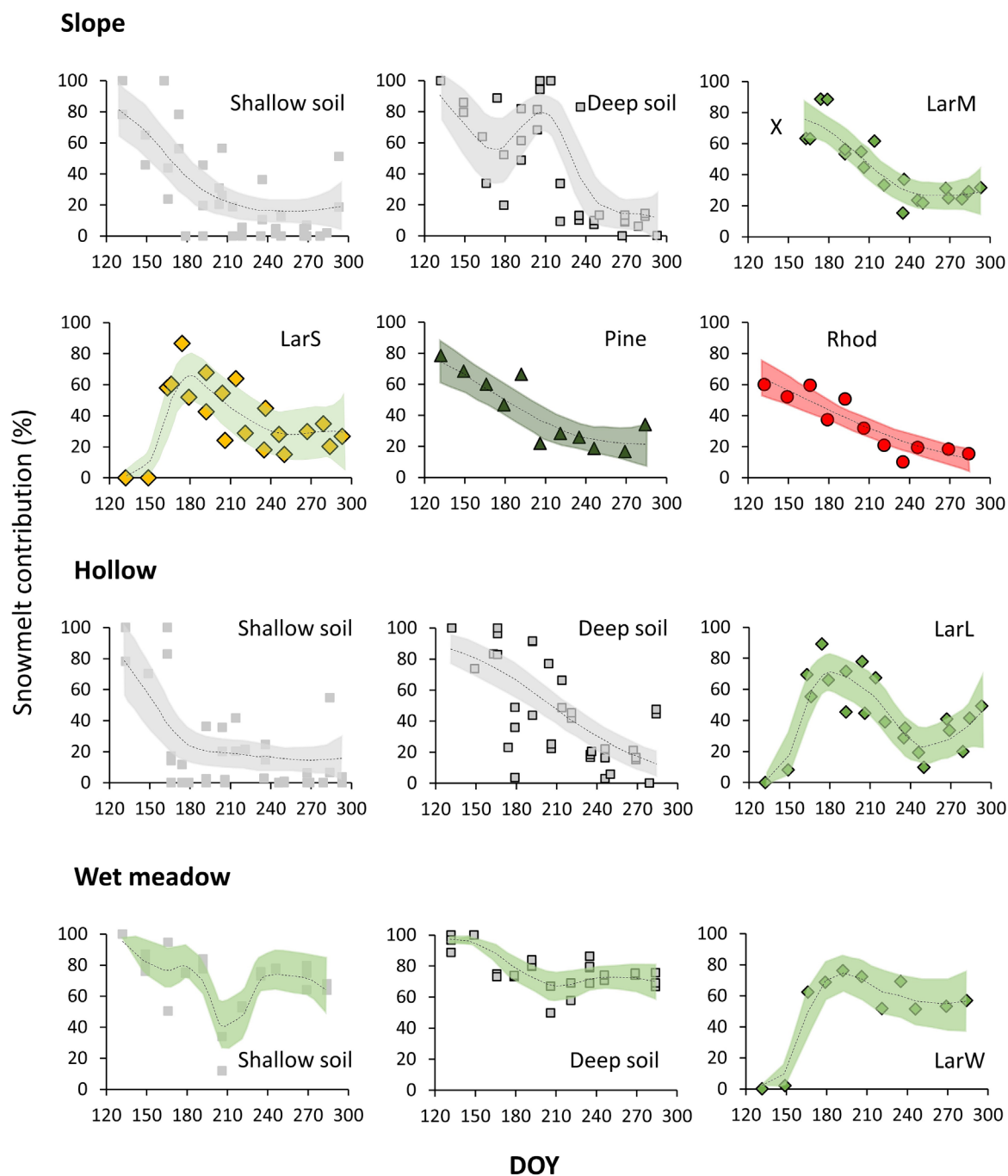


**FIGURE 6** Scatterplots of day of the year (DOY) and snowmelt contribution at soil depths and trees from different locations. Coloured shades represent GAMs fitted to the data (without the covariate year; see Data S2 for the model outcomes and specifications).

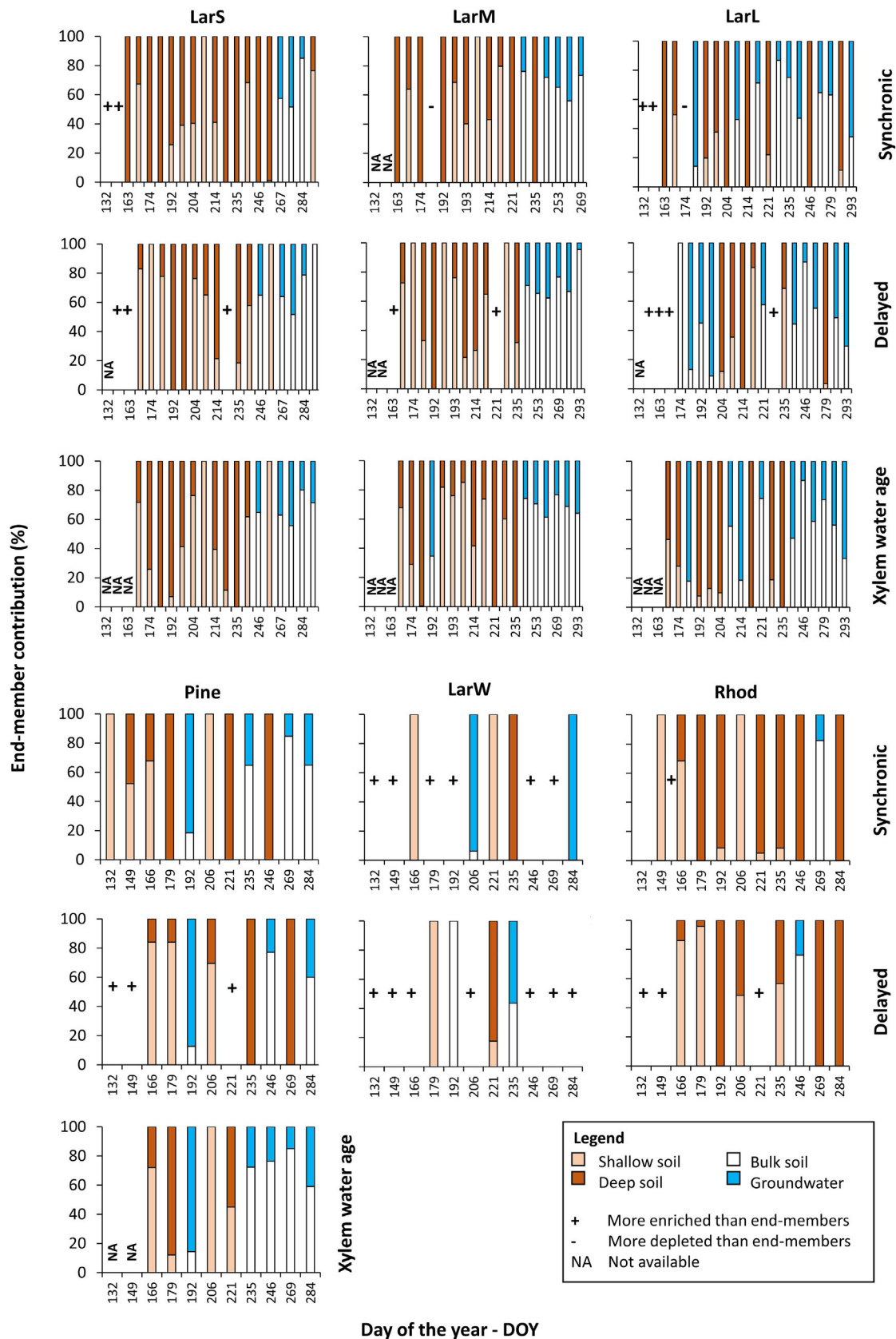


**FIGURE 7** End-member contribution to xylem waters of different plants during each sampling, over a DOY gradient. If xylem water was more depleted in  $\delta^{18}\text{O}$  than the most depleted soil water sample, soil/groundwater contributions were calculated. If xylem signature was more enriched (+) or depleted (-) than any end-member value, mixing models could not be performed.

was recorded (Figure 2c). The xylem water of LarW was more depleted in heavy isotopes than that of larch trees located at the slope and the hollow. On seven occasions, the isotopic values of xylem water were outside the range of the soil water at the wet meadow and intermediate between the soil at this location and those at the slope/hollow (Figures 4 and 5). The xylem water of Pine and Rhod was generally more enriched in heavy isotopes than that of larch trees, except for the early season.

### 3.4 | Snowmelt contribution to different water pools

Rainfall ( $-8.8 \pm 2.1\%$ ,  $n = 18$ ) and snowmelt ( $-16.9 \pm 0.7\%$ ,  $n = 15$ ) had significantly different values of  $\delta^{18}\text{O}$  ( $p < 0.001$ ; Figure 4). According to MixSiar analyses, the snowmelt contribution was highest at the wet meadow system ( $73.9 \pm 5.2\%$ ) than at the slope ( $37.8 \pm 2.6\%$ ) and at the hollow ( $34.9 \pm 3.0\%$ ). In the latter two locations, the snowmelt contribution was higher in the xylem ( $45.2 \pm 2.9\%$ ) and the deep soil ( $40.9 \pm 3.5\%$ ) water than in the shallow soil water ( $23.6 \pm 3.8\%$ ). When considering the seasonal variability of snowmelt contribution, the comparison of different continuous covariates highlighted the variable 'day of the year' as a better explanatory variable over 'day after snowmelt' and 'day after leaf out', with the Akaike weight indicating 74% of probability that including DOY would return the best model (Data S2). Also GAMs, performed using single mixture values (uncertainties of  $10.6 \pm 3.6\%$ ), highlighted DOY as a stronger smooth term for the snowmelt contribution (Data S4). Overall, 'year' was a significant covariate in the models with lower snowmelt contribution during summer 2021 than that of 2020 (Data S4).

The snowmelt contribution to soil water showed a sharp seasonality, with peak values in May, a decreasing proportion as summer

progressed and a return to some snowmelt contribution in October. The seasonal decrease of snowmelt contribution was more evident and quicker in the shallow than in the deeper soil and in the hollow (Figure 6). A transient rise of the snowmelt contribution, more evident at the slope than at the hollow, occurred in soil water during July/August, after 7–10 days of dry conditions or soon after rain/snow or hail events. At the wet meadow, after the progressive depletion of snowmelt contribution during May and June, the soil water signature stabilised around a 65–75% of snowmelt contribution, in rough agreement with that of freshwaters. This phenomenon was particularly evident for the deeper soil (Figure 5). At each location, the seasonal contribution of the snowmelt in xylem water reflected that of the soil water with decreasing values as summer progressed. In contrast to these common trends, samples from the early growing season of larch trees exhibited a low/absent snowmelt contribution but later increased in June (Figure 6).

### 3.5 | Xylem water components under different travel time scenarios

The applied mixing models of soil/groundwater contribution to xylem water provided slightly contrasting outcomes, depending on the tree and on the scenario considered (Figure 7). Overall, the uncertainty of the model outcomes was in the range of 1–11.5% (Data S5). The isotopic signature of xylem water was consistent with the use of a mixture of shallow and deep soil water by the plants during most of the sampling dates. When compared with the synchronic one, the xylem water age scenario had a larger number of samples where groundwater contribution had to be considered (Table 2; Figure 8). This occurred a higher number of times LarL, followed by LarM and Pine, and by LarS and Rhod (Figure 8a). Groundwater contribution had to

	Synchronic	Xylem water age	Delayed
Upper (vs. lower) soil	35 ± 38	43 ± 35%	49 ± 38%
LarS	31 ± 34	45 ± 37	55 ± 38
LarM	35 ± 36	46 ± 35	56 ± 36
LarL	16 ± 18	15 ± 16	34 ± 35
Pine	46 ± 46	57 ± 38	48 ± 44
Rhod	32 ± 44	na	41 ± 42
LarW	67 ± 58	na	59 ± 58
Groundwater (vs. bulk soil)	11 ± 23%	15 ± 23%	12 ± 22%
LarS	5 ± 14%	7 ± 15	7 ± 15
LarM	10 ± 15	9 ± 15	9 ± 15
LarL	19 ± 27	24 ± 32	24 ± 33
Pine	15 ± 26	13 ± 28	14 ± 28
Rhod	2 ± 5	na	2 ± 7
LarW	18 ± 40	na	5 ± 18

**TABLE 2** Comparison of the outcomes from different mixing modelling scenarios: synchronic, xylem water age and delayed.

**Note:** The leaf out period was discarded because the old ages of the xylem water hindered the calculations for the delayed and xylem water age scenarios. The statistics were obtained considering zero values of groundwater contribution when the shallow and deep soil waters were accounted for.

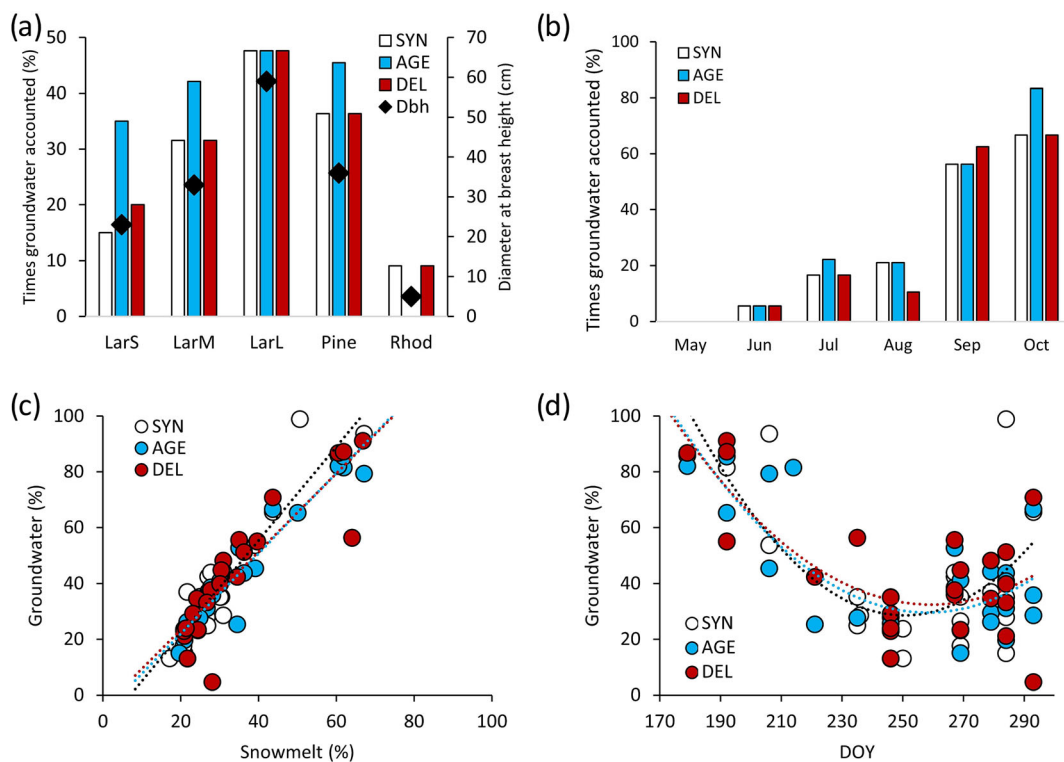


**FIGURE 8** Relation between key variables and groundwater (calculated against bulk soil water) contribution to xylem water. Percentage of times that groundwater contribution was accounted: (a) for each tree; the size of each tree is related to its diameter at breast height, except for Rhod for which we considered the diameter of the base trunk; (b) during each month, over the total of xylem water samples. Contribution of groundwater to xylem water as a function of (c) snowmelt (calculated against rainwater) contribution to xylem water (linear regression lines are fitted) and (d) DOY (with fitted polynomial equations,  $k = 2$ ). Note: We only show those samples for which groundwater contribution was considered. SYN = synchronic scenario; AGE = xylem water age scenario; DEL = delayed scenario.

be considered a higher number of times when moving towards the end of the growing season (Figure 8b). When it was accounted for, the groundwater (vs. bulk soil) contribution was strongly related to the snowmelt contribution (Figure 8c) and decreased during the growing season (Figure 8d). For all plants, early season xylem water was more enriched in heavy isotopes than the dominant end-member water for at least two scenarios (Figure 7). Most of LarW xylem water samples was more enriched in heavy isotopes when compared with groundwater and the soil waters belonging to the wet meadow. Pine and Rhod had a progressive decrease of the shallow water contribution as summer progressed, except right after rain events (not shown), and a progressive increase of the deep soil water contribution or the use of groundwater.

## 4 | DISCUSSIONS

### 4.1 | Ecohydrological setting of the subalpine forest: A conceptual model

Landscape topography on steep slopes often entails a large heterogeneity in substrate morphology and soil texture, both influencing soil

water content and therefore the water uptake by plants (e.g., Brooks et al., 2015; Dick et al., 2018; Fabiani et al., 2021; Nardini et al., 2021). The investigated subalpine coniferous forest was characterised by a slope/hollow conformation with a complex architecture of the subsurface (Figure 9a). Along the hollow, a ‘ramp-like’ morphology underlying the upper soil layers, made of compacted sediments, acted as an aquitard conveying groundwater towards the wet meadow and to the springs. Consequently, the isotopic fingerprint of the soil water in this area was very similar to that of the spring water. Differently, at the hollow and the slope, the soil water was not influenced by groundwater, as testified by different isotopic conditions when compared with those of the wet meadow. However, plants were only slightly influenced by the sharp isotopic differences in the soil between the two areas (Figure 5). Indeed, the xylem water of larch trees located at the slope/hollow only slightly differed from that of the larch located at the wet meadow. Plants located on very wet soils should cope with physical constraints (e.g., anoxic conditions), even limiting their rooting depth (Fan et al., 2017). Thus, plants that are not physiologically pre-adapted to these limiting factors preferentially use water from the vadose zone (Engel et al., 2022; Fabiani et al., 2021). At Matscher Alm, the larch tree at the wet meadow was also very close (2 m) to the slope. Hence, not surprisingly, we found evidence

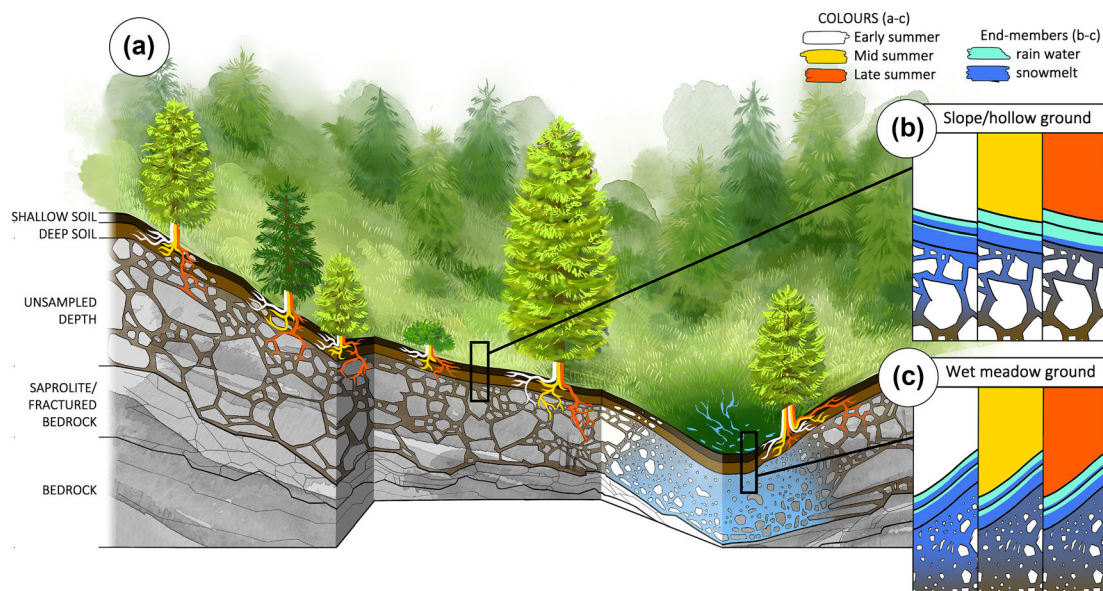


**FIGURE 9** Conceptual model of the Matscher Alm critical zone. The subsurface heterogeneity of the area influences the use of water by trees. During different timings of the season, trees tend to transpire different types of water. Soon after the leaf out of larches, the water in the ground is highly available, and the snowmelt component is large (b,c). Consequently, trees take up water from a mixture of shallow and deeper soil (a). As summer progresses, the snowmelt component of the soil water gradually fades out and more quickly at shallow depths (b). Therefore, trees increasingly use deeper water resources in the ground, where water is more available. The use of water from the deep ground ('unsampled depth') is higher for larger plants (a). By contrast, at the wet meadow location (c), trees use a combination of saturated zone and slope water. Since the soil water at the wet meadow has a large snowmelt component, its contribution to tree transpiration remains large even during late summer. Credits: Vanessa Arrighi.

of root water uptake from both areas, as suggested by the intermediate isotopic values of xylem water between those of the wet meadow and those of the slope/hollow soils.

The isotopic variability of soil and xylem water was strongly dictated by seasonal dynamics (Figure 9). Within the soil, water from shallow depths had a quicker isotopic enrichment as summer progressed, when compared with that from the deep soil. This can be explained with a more efficient mixing of precipitation events occurring during the early season in the shallow soil and a slower consecutive water mixing in the deep soil (Sprenger et al., 2016). Even though a similar isotopic enrichment was also observed seasonally for the xylem water, there was an isotopic mismatch between the soil and the xylem water for larch trees during the period of leaf out. During this stage, sap velocities were very low in larch trees ( $\text{cm day}^{-1}$ ), and the calculated xylem water ages were in the order of 100–250 calendar days. This suggests the use of previously stored water reserves for this species during the leaf out, as demonstrated by Nehemy et al. (2022) in a boreal coniferous forest. However, different processes may be responsible for isotopic enrichment in the xylem water during winter. For example, Losso et al. (2021) found evidence of atmospheric moisture absorption by branches in *L. decidua* and *Picea abies* in a subalpine forest. We did not find evidence of a similar isotopic mismatch for the stone pine and for the alpenrose during the early growing season. This agrees with observations from a coniferous mountain forest in China, where Zhang et al. (2021) found a larger contribution of internal storage in deciduous larch trees than in

evergreen spruce trees during the early phenological stages. Indeed, evergreen gymnosperms can start transpiration before the end of snow cover (Bowling et al., 2018; Chan & Bowling, 2017; Lehner & Lütz, 2003; Nehemy et al., 2022) and thus weeks before the seasonal onset of transpiration by larch trees (Nehemy et al., 2022).

## 4.2 | Snowmelt contribution to different water pools

At high elevations, precipitation occurs as snowfall during wintertime and, occasionally, also during summer. Even though the isotopic signature of precipitation typically has a sinusoidal behaviour imparted by climatic seasonality (e.g., Allen et al., 2019), only a very frequent (e.g., event scale) sampling of precipitation can help discriminate the snow and rainfall fractions of precipitation. Given the sampling frequency (bi-weekly) of our investigations, we could not distinguish snow and rain water fractions, and therefore, we used rainfall and snowmelt end-members with fixed rather than time-variant values in mixing models. Even the snowmelt signature can have a strong spatial and temporal variability (e.g., Lee et al., 2010; Engel et al., 2016; Schmieler et al., 2016; Beria et al., 2018; Zuecco et al., 2019), but the relatively quick freshet occurring at a small scale (which also allowed collecting snowmelt water only on a few occasions) suggests that this variability may not be important for the isotopic composition of soil water in the plot.

We found that snowmelt accounted for 75–80% of discharge at the springs and the stream, with a very low seasonality. A similarly high snowmelt contribution in soil water at the wet meadow (50–70%) can be explained with the seepage of the spring water into the ground (Figure 9c). Among all plants, the larch located at the wet meadow had a higher share of snowmelt contribution to xylem water, particularly during the second half of summer when this component declined in the other plants but remained stable at 45–50% for this tree. In a previous study carried out in a mountain environment in China, Zhu et al. (2022) found that the snowmelt contribution to soil and plant water rose during early summer (up to 60–70%) and gradually faded out towards autumn (down to 10%) and that there was a consistency between the fraction of snowmelt/rainfall in the soil and in the xylem waters. Similarly, in our work, the snowmelt component in the upper part of the plot peaked during early summer (up to 70–100%) and decreased towards autumn, and we found a more pronounced and quicker drop in the shallow than in the deeper soil. In the latter, we detected a transient increase of snowmelt contribution during some sampling (Figure 9b). This transient pulse, occurring during the period of major water deficit (July) and more evident at the slope than at the hollow, might be related to the uplift of deeper (and not investigated, see below) water resources, where the snowmelt component would be larger. Key processes such as groundwater table uplift, capillary rise (Orlowski et al., 2016) or water redistribution by roots (Prieto et al., 2012; Wei et al., 2022) can be important drivers of vertical rearrangements of the soil water (Sprenger et al., 2016), even in coniferous forests (Warren et al., 2007). However, we did not investigate these mechanisms that can only be hypothesised to occur in the study area.

While most of the plants had a relatively constant and low (10–20%) snowmelt contribution during September/October, the same component increased for xylem water of the large and medium sized larches and for the stone pine, during the same period. A contribution from meltwater from recent snowfall events can explain this behaviour, because a similar increase of snowmelt contribution was found for the soil at the hollow. During the same period, the same pattern was not detected at the slope, likely because (i) a higher canopy cover hindering the snow to reach the soil at the slope and/or (ii) lower snow accumulation/persistence than in the hollow.

The complex interplay between location in the plot and the use of different ground compartments by the plants might have been responsible for the fluctuating behaviour of the snowmelt component superimposing on the seasonal trend. This contrasts with the steady pattern observed by Zhu et al. (2022) in China, where soil was homogeneous and deep, and the occurrence of a rainy season enhanced the dilution effect from successive rainfall events at depth.

Unexpectedly, the calendar day was a stronger explanatory variable for the snowmelt contribution in GAMs, when compared with the time elapsed after the snow cover ended. Snowfall events occurred after the end of winter snow cover during early summer 2020. These events only slightly (15–16 mm) and transiently (3–5 h) made the snow pack to rise at the meteorological station (and thus are not displayed in Figure 2) and provided additional snowmelt

recharge to the ground. Similar early summer snowfall events did not occur in 2021, when—not surprisingly—the snowmelt component in the xylem and the soil water was slightly lower than in 2020 according to GAM analyses. This again testifies the difficulty to distinguish the water from the solid and liquid fractions of precipitation in alpine environments.

### 4.3 | Xylem water components under different travel time scenarios

Among the different travel time scenarios used to investigate the relative contribution of water from different soil depths to tree transpiration, only the one accounting for the xylem water age returned all mixture samples in the range of their potential water sources. Hence, this method can be hypothesised as the most valuable to inform end-member characterisation in mixing models. Nonetheless, we used a simplistic method that, for example, assumed unidirectional sap fluxes and considered the isotopic composition of soil water as a linear combination between antecedent and posterior periods. Yet, accounting for travel times seems to be crucial for gymnosperms, given the magnitude (weeks to months) of the xylem water age (Tetzlaff et al., 2020). For example, preliminary sap flow data may be used to plan delayed sampling of soil water and xylem water.

Despite clear differences in percentage values of end-member contribution, all travel time scenarios converged to a high likelihood of deep soil and groundwater use by plants. This was particularly evident during late summer, when the snowmelt water reservoir was depleted, and the upper soil was drier compared to the early growing season. A greater use of groundwater by larger plants may be explained by a deeper rooting system compared to smaller plants. In the Canadian Rockies, a higher use of deep soil water by older trees than by younger ones was attributed to the contrasting root development at different depths (Langs et al., 2019). Similarly, Xu et al. (2011) found a strong relationship between fine root distribution and the use of groundwater resources in a Chinese subalpine forest. Unfortunately, we did not investigate the root distribution of the studied trees and cannot build on these findings.

### 4.4 | Groundwater as surrogate for an unsampled end-member

In this work, we justified more negative isotope values of xylem water than those of the shallow and deep soil water with the possible use of groundwater by the plants. Unlike at the wet meadow location, where the presence of (spring) groundwater in the soil was evident, the groundwater component was only a surrogate of an unsampled water resource at the slope and the hollow (Figure 9a). Indeed, the saturated zone was most likely too deep (>5 m) to be accessible by the roots, as revealed by the geophysical surveys. The excavation of a small trench at the slope (performed after conducting this study) revealed the presence (below 30–50 cm) of a matrix of fine sediment, fractured

bedrock and soil including abundant stones and boulders. While the roots of the investigated plants could easily penetrate the interstices among medium and large rocky clasts of this ground, our gravity corer could not. For this reason, the isotopic composition of water from this depth interval was not assessed, as different and more invasive sampling strategies would have been required (e.g., trenches at key locations). This deep water at the intersection between the soil and the regolith is hypothesised to cover the entire slope and the upper part of the hollow, as suggested by geophysical surveys. In general, this water may be important for forests located in similar mountain terrains, as demonstrated for the rock moisture (Rempe & Dietrich, 2018) and its significance for plants transpiration (Hahm et al., 2020).

## 5 | CONCLUSIONS

Our work represents the first tracer-based characterisation of a sub-alpine coniferous forest in the Italian Alps. To the best of our knowledge, we offered a first attempt to use the outcomes of geophysical surveys to aid the interpretation of the isotopic results. This combined approach helped shape the conceptual model of the Critical Zone in the study area, to be corroborated by future specific studies. These might include boreholes validating the internal structure of the ground, the monitoring of the spatio-temporal dynamics of the shallow groundwater, increasing the number of investigated plants and soil sampling locations and hydrological modelling of water distribution in the soil profile. All these integrated methods may support our findings on the relation between a large subsurface heterogeneity and the isotopic composition in the soil and xylem water at high elevations where snowmelt is a key ecohydrological driver. Outside wet areas, the snowmelt component rapidly fades out in the shallow soil after the freshet, but it persists until late summer in the deep soil. The seasonal decrease of the snowmelt component in xylem water is dampened by the complex use of different ground compartments by the plants. The use of deep water sources, including those from a potential 'stoney ground moisture', is higher for larger plants and, for each plant, during late summer. By comparing different modelling frameworks, we found evidence that the isotopic mismatch between soil and xylem water can be caused by long sap travel times. Our study represents a first preliminary attempt to consider these travel times when estimating the depths of root water uptake, which needs confirmation by additional independent evidence.

## ACKNOWLEDGEMENTS

This research was supported by the PRIN MIUR 2017SL7ABC\_005 WATZON (Water mixing in the critical zone) project. We thank Rudi Nadalet and the Autonomous Province of Bolzano/Bozen for unpublished lithological map (CARG, Foglio 12 - Silandro); Edoardo Bortolotti, Andrea Andreoli and Johannes Holzner for their precious help in the field; and Vanessa Arrighi for the development of the conceptual model artwork.

## DATA AVAILABILITY STATEMENT

The data that support the findings of this study are available from the corresponding author upon reasonable request.

## ORCID

Stefano Brighenti  <https://orcid.org/0000-0001-6111-2311>

Giulia Zuecco  <https://orcid.org/0000-0002-2125-0717>

Daniele Penna  <https://orcid.org/0000-0001-6915-0697>

Francesco Comiti  <https://orcid.org/0000-0001-9840-0165>

## REFERENCES

- Allen, S. T., Kirchner, J. W., Braun, S., Siegwolf, R. T. W., & Goldsmith, G. R. (2019). Seasonal origins of soil water used by trees. *Hydrology and Earth System Sciences*, 23, 1199–1210. <https://doi.org/10.5194/hess-23-1199-2019>
- Amin, A., Zuecco, G., Marchina, C., Engel, M., Penna, D., McDonnell, J. J., & Borgia, M. (2021). No evidence of isotopic fractionation in olive trees (*Olea europaea*): A stable isotope tracing experiment. *Hydrological Sciences Journal*, 66(16), 2415–2430. <https://doi.org/10.1080/02626667.2021.1987440>
- Autonomous Province of Bolzano/Bozen [APB]. (2022). Online Geobrowser v.3. <https://maps.civis.bz.it/>
- Autonomous Province of Bozen/Bolzano [APB]. (2023). Carta geologica d'Italia scala 1:50000, Foglio 012 - Silandro. In production.
- Bachofen, C., Poyatos, R., Flo, V., Martínez-Vilalta, J., Mencuccini, M., Granda, V., & Grossiord, C. (2023). Stand structure of central European forests matters more than climate for transpiration sensitivity to VPD. *Journal of Applied Ecology*, 60, 886–897. <https://doi.org/10.1111/1365-2664.14383>
- Barbeta, A., Jones, S. P., Clavé, L., Wingate, L., Gimeno, T. E., Fréjaville, B., Wohl, S., & Ogée, J. (2019). Unexplained hydrogen isotope offsets complicate the identification and quantification of tree water sources in a riparian forest. *Hydrology and Earth System Sciences*, 23(4), 2129–2146. <https://doi.org/10.5194/hess-23-2129-2019>
- Barbeta, A., & Peñuelas, J. (2017). Relative contribution of groundwater to plant transpiration estimated with stable isotopes. *Scientific Reports*, 7(1), 10580. <https://doi.org/10.1038/s41598-017-09643-x>
- Beniston, M. (2003). Climatic change in mountain regions: A review of possible impacts. *Climatic Change*, 59, 5–31. <https://doi.org/10.1023/A:1024458411589>
- Beria, H., Larsen, J. R., Ceperley, N. C., Michelon, A., Vennemann, T., & Schaeffli, B. (2018). Understanding snow hydrological processes through the lens of stable water isotopes. *WIREs Water*, 5, e1311. <https://doi.org/10.1002/wat2.1311>
- Bertoldi, G., Bozzoli, M., Crespi, A., Matiu, M., Giovannini, L., Zardi, D., & Majone, B. (2023). Diverging snowfall trends across months and elevation in the northeastern Italian Alps. *International Journal of Climatology*, 43(6), 2794–2819. <https://doi.org/10.1002/joc.8002>
- Beyer, M., & Penna, D. (2021). On the Spatio-temporal underrepresentation of isotopic data in ecohydrological studies. *Frontiers in Water*, 3, 643013. <https://doi.org/10.3389/frwa.2021.643013>
- Blanchy, G., Saneiyani, S., Boyd, J., McLachlan, P., & Binley, A. (2020). ResIPy, an intuitive open source software for complex geoelectrical inversion/modelling. *Computers & Geosciences*, 137, 104423. <https://doi.org/10.1016/j.cageo.2020.104423>
- Bowling, D. R., Logan, B. A., Hufkens, K., Aubrecht, D. M., Richardson, A. D., Burns, S. P., Anderegg, W. R. L., Blanken, P. D., & Eiriksson, D. P. (2018). Limitations to winter and spring photosynthesis of a Rocky Mountain subalpine forest. *Agricultural and Forest Meteorology*, 252, 241–255. <https://doi.org/10.1016/j.agrformet.2018.01.025>
- Brinkmann, N., Seeger, S., Weiler, M., Buchmann, N., Eugster, W., & Kahmen, A. (2018). Employing stable isotopes to determine the



- residence times of soil water and the temporal origin of water taken up by *Fagus sylvatica* and *Picea abies* in a temperate forest. *New Phytologist*, 219, 1300–1313. <https://doi.org/10.1111/nph.15255>
- Brooks, P. D., Chorover, J., Fan, Y., Godsey, S. E., Maxwell, R. M., McNamara, J. P., & Tague, C. (2015). Hydrological partitioning in the critical zone: Recent advances and opportunities for developing transferable understanding of water cycle dynamics. *Water Resources Research*, 51, 6973–6987. <https://doi.org/10.1002/2015WR017039>
- Cermak, J., Kucera, J., & Nadezhdina, N. (2004). Sap flow measurements with some thermodynamic methods, flow integration within trees and scaling up from sample trees to entire forest stands. *Trees*, 18, 529–546. <https://doi.org/10.1007/s00468-004-0339-6>
- Chan, A. M., & Bowling, D. R. (2017). Assessing the thermal dissipation sap flux density method for monitoring cold season water transport in seasonally snow-covered forests. *Tree Physiology*, 37, 984–995. <https://doi.org/10.1093/treephys/tpx049>
- Christensen, C. W., Hayashi, M., & Bentley, L. R. (2020). Hydrogeological characterization of an alpine aquifer system in the Canadian Rocky Mountains. *Hydrogeology Journal*, 28, 1871–1890. <https://doi.org/10.1007/s10040-020-02153-7>
- Colombo, N., Guyennon, N., Valt, M., Salerno, F., Godone, D., Cianfarra, P., Freppaz, M., Maugeri, M., Manara, V., Acquaotta, F., Petrangeli, A. B., & Romano, E. (2023). Unprecedented snow-drought conditions in the Italian Alps during the early 2020s. *Environmental Research Letters*, 18(7), 074014. <https://doi.org/10.1088/1748-9326/acdb88>
- Cui, J., Tian, L., Gerlein-Safdi, C., & Qu, D. (2017). The influence of memory, sample size effects, and filter paper material on online laser-based plant and soil water isotope measurements. *Rapid Communications in Mass Spectrometry*, 31, 509–522. <https://doi.org/10.1002/rcm.7824>
- Dick, J., Tetzlaff, D., Bradford, J., & Soulsby, C. (2018). Using repeat electrical resistivity surveys to assess heterogeneity in soil moisture dynamics under contrasting vegetation types. *Journal of Hydrology*, 559, 684–697. <https://doi.org/10.1016/j.jhydrol.2018.02.062>
- Dolezal, J., Kurnotova, M., Stastna, P., & Klimesova, J. (2020). Alpine plant growth and reproduction dynamics in a warmer world. *New Phytologist*, 228, 1295–1305. <https://doi.org/10.1111/nph.16790>
- Dubbert, M., Caldeira, M. C., Dubbert, D., & Werner, C. (2019). A pool-weighted perspective on the two-water-worlds hypothesis. *New Phytologist*, 222, 1271–1283. <https://doi.org/10.1111/nph.15670>
- Engel, M., Frentress, J., Penna, D., Andreoli, A., van Meerveld, I., Zerbe, S., Tagliavini, M., & Comiti, F. (2022). How do geomorphic characteristics affect the source of tree water uptake in restored river floodplains? *Ecohydrology*, 15(4), e2443. <https://doi.org/10.1002/eco.2443>
- Engel, M., Penna, D., Bertoldi, G., Dell'Agnese, A., Soulsby, C., & Comiti, F. (2016). Identifying run-off contributions during melt-induced run-off events in a glacierized alpine catchment. *Hydrological Processes*, 30, 343–364. <https://doi.org/10.1002/hyp.10577>
- Evaristo, J., & McDonnell, J. J. (2017). Prevalence and magnitude of groundwater use by vegetation: A global stable isotope meta-analysis. *Scientific Reports*, 7(44110), 44110. <https://doi.org/10.1038/srep44110>
- Fabiani, G., Penna, D., Barbata, A., & Klaus, J. (2022). Sapwood and heartwood are not isolated compartments: Consequences for isotope ecohydrology. *Ecohydrology*, 15(8). <https://doi.org/10.1002/eco.2478>
- Fabiani, G., Schoppach, R., Penna, D., & Klaus, J. (2021). Transpiration patterns and water use strategies of beech and oak trees along a hillslope. *Ecohydrology*, 15(2), e2382. <https://doi.org/10.1002/eco.2382>
- Fan, Y., Miguez-Macho, G., Jobbágy, E. G., Jackson, R. B., & Otero-Casal, C. (2017). Hydrologic regulation of plant rooting depth. *Proceedings of the National Academy of Sciences of the United States of America*, 114, 10572–10577. <https://doi.org/10.1073/pnas.1712381114>
- Genereux, D. (1998). Quantifying uncertainty in tracer-based hydrograph separations. *Water Resources Research*, 34(4), 915–919. <https://doi.org/10.1029/98wr00010>
- Giuliani, N., Aguzzoni, A., Penna, D., & Tagliavini, M. (2023). Estimating uptake and internal transport dynamics of irrigation water in apple trees using deuterium-enriched water. *Agricultural Water Management*, 289, 108532. <https://doi.org/10.1016/j.agwat.2023.108532>
- Hahm, W. J., Rempe, D. M., Dralle, D. N., Dawson, T. E., & Dietrich, W. E. (2020). Oak transpiration drawn from the weathered bedrock vadose zone in the summer dry season. *Water Resources Research*, 56, e2020WR027419. <https://doi.org/10.1029/2020WR027419>
- Harrington, J. S., Mozil, A., Hayashi, M., & Bentley, L. R. (2018). Groundwater flow and storage processes in an inactive rock glacier. *Hydrological Processes*, 32, 3070–3088. <https://doi.org/10.1002/hyp.13248>
- Hayashi, M. (2019). Alpine hydrogeology: The critical role of groundwater in sourcing the headwaters. *Groundwater*, 58, 498–510. <https://doi.org/10.1111/gwat.12965>
- Hock, R., Rasul, G., Adler, C., Cáceres, B., Gruber, S., Hirabayashi, Y., Jackson, M., Käbb, A., Kang, S., Kutuzov, S., & Milner, A. (2019). High mountain areas. In H. O. Pörtner, D. C. Roberts, V. Masson-Delmotte, P. Zhai, M. Tignor, E. Poloczanska, K. Mintenbeck, A. Alegria, M. Nicolai, A. Okem, J. Petzold, B. Rama, & N. M. Weyer (Eds.), *IPCC special report on the ocean and cryosphere in a changing climate*. Cambridge University Press, Cambridge, UK and New York, NY, USA, pp. 131–202. <https://doi.org/10.1017/9781009157964.004> [https://www.ipcc.ch/site/assets/uploads/sites/3/2019/11/06\\_SROCC\\_Ch02\\_FINAL.pdf](https://www.ipcc.ch/site/assets/uploads/sites/3/2019/11/06_SROCC_Ch02_FINAL.pdf)
- IBM. (2018). SPSS Statistics software, v.27
- Kirchner, J. W., Benettin, B., & van Meerveld, I. (2023). Instructive surprises in the hydrological functioning of landscapes. *Annual Review of Earth and Planetary Sciences*, 51(1), 277–299. <https://doi.org/10.1146/annurev-earth-071822-100356>
- Koeniger, P., Marshall, J. D., Link, T., & Mulch, A. (2011). An inexpensive, fast, and reliable method for vacuum extraction of soil and plant water for stable isotope analyses by mass spectrometry. *Rapid Communications in Mass Spectrometry*, 25, 3041–3048. <https://doi.org/10.1002/rcm.5198>
- Kučera, J. (2010). EMS 62 sap flow system for small stems or branches. Environmental Measuring System Turistická 5, 621 00 BRNO, Czech Republic. [https://katedry.czu.cz/storage/182/4309\\_1\\_sap\\_flow\\_system\\_instruction\\_manual.pdf](https://katedry.czu.cz/storage/182/4309_1_sap_flow_system_instruction_manual.pdf)
- Landgraf, J., Tetzlaff, D., Dubbert, M., Dubbert, D., Smith, A., & Soulsby, C. (2022). Xylem water in riparian willow trees (*Salix alba*) reveals shallow sources of root water uptake by in situ monitoring of stable water isotopes. *Hydrology and Earth Systems Sciences*, 26, 2073–2092. <https://doi.org/10.5194/hess-26-2073-2022>
- Landwehr, J., & Coplen, T. B. (2006). Line-conditioned excess: A new method for characterizing stable hydrogen and oxygen isotope ratios in hydrologic systems. In *Isotopes in environmental studies, aquatic forum 2004* (pp. 132–135). International Atomic Energy Agency, IAEA-CSP26.
- Langs, L. E., Petrone, R. M., & Pomeroy, J. W. (2019). A  $\delta^{18}\text{O}$  and  $\delta^2\text{H}$  stable water isotope analysis of subalpine forest water sources under seasonal and hydrological stress in the Canadian Rocky Mountains. *Hydrological Processes*, 2020(34), 5642–5658. <https://doi.org/10.1002/hyp.13986>
- Lee, J., Feng, X., Faiia, A., Posmentier, E., Osterhuber, R., & Kirchner, J. (2010). Isotopic evolution of snowmelt: A new model incorporating mobile and immobile water. *Water Resources Research*, 46, W11512. <https://doi.org/10.1029/2009WR008306>
- Lehner, L., & Lütz, C. (2003). Photosynthetic functions of cembran pines and dwarf pines during winter at timberline as regulated by different temperatures, snowcover and light. *Journal of Plant Physiology*, 160(2), 153–166. <https://doi.org/10.1078/0176-1617-00798>

- Losso, A., Bär, A., Unterholzner, L., Unterholzner, L., Bahn, M., & Mayr, S. (2021). Branch water uptake and redistribution in two conifers at the alpine treeline. *Scientific Reports*, 11, 22560. <https://doi.org/10.1038/s41598-021-00436-x>
- Migliavacca, M., Cremonese, E., Colombo, R., Busetto, L., Galvagno, M., Ganis, L., Meroni, M., Pari, E., Rossini, M., Siniscalco, C., & Morra di Cella, U. (2008). European larch phenology in the Alps: Can we grasp the role of ecological factors by combining field observations and inverse modelling? *International Journal of Biometeorology*, 52(7), 587–605. <https://doi.org/10.1007/s00484-008-0152-9>
- Miguez-Macho, G., & Fan, Y. (2021). Spatiotemporal origin of soil water taken up by vegetation. *Nature*, 598(7882), 624–628. <https://doi.org/10.1038/s41586-021-03958-6>
- Millar, C., Janzen, K., Nehemy, M. F., Koehler, G., Hervé-Fernández, P., Wang, H., Orłowski, N., Barbeta, A., & McDonnell, J. J. (2022). On the urgent need for standardization in isotope-based ecohydrological investigations. *Hydrological Processes*, 36(10). <https://doi.org/10.1002/hyp.14698>
- Nardini, A., Petruzzellis, F., Marusig, D., Tomasella, M., Natale, S., Altobelli, A., Calligaris, C., Floriddia, G., Cucchi, F., Forte, E., & Zini, L. (2021). Water 'on the rocks': A summer drink for thirsty trees? *New Phytologist*, 229, 199–212. <https://doi.org/10.1111/nph.16859>
- Nehemy, M. F., Maillet, J., Perron, N., Pappas, C., Sonnentag, O., Baltzer, J. L., Laroque, C. P., & McDonnell, J. J. (2022). Snowmelt water use at transpiration onset: Phenology, isotope tracing, and tree water transit time. *Water Resources Research*, 58, e2022WR032344. <https://doi.org/10.1029/2022WR032344>
- Obojes, N., Meurer, A., Newesely, C., Tasser, E., Oberhuber, W., Mayr, S., & Tappeiner, U. (2018). Water stress limits transpiration and growth of European larch up to the lower subalpine belt in an inner-alpine dry valley. *The New Phytologist*, 220, 460–475. <https://doi.org/10.1111/nph.15348>
- Obojes, N., Meurer, A. K., Newesely, C., Tasser, E., Oberhuber, W., Mayr, S., & Tappeiner, U. (2022). Swiss stone pine growth benefits less from recent warming than European larch at a dry-inner alpine forest line as it reacts more sensitive to humidity. *Agricultural and Forest Meteorology*, 315, 108788. <https://doi.org/10.1016/j.agrformet.2021.108788>
- Orłowski, N., Kraft, P., Pferdmeiges, J., & Breuer, L. (2016). Exploring water cycle dynamics by sampling multiple stable water isotope pools in a developed landscape in Germany. *Hydrology and Earth Systems Sciences*, 20, 3873–3894. <https://doi.org/10.5194/hess-20-3873-2016>
- Oshun, J., Dietrich, W. E., Dawson, T. E., & Fung, I. (2016). Dynamic, structured heterogeneity of water isotopes inside hillslopes. *Water Resources Research*, 52(1), 164–189. <https://doi.org/10.1002/2015WR017485>
- Penna, D., Engel, M., Mao, L., Dell'Agnese, A., Bertoldi, G., & Comiti, F. (2014). Tracer-based analysis of spatial and temporal variations of water sources in a glacierized catchment. *Hydrology and Earth Systems Sciences*, 18, 5271–5288. <https://doi.org/10.5194/hess-18-5271-2014>
- Penna, D., Stenni, B., Šanda, M., Wrede, S., Bogaard, T. A., Michelini, M., Fischer, B. M. C., Gobbi, A., Mantese, N., Zuecco, G., Borga, M., Bonazza, M., Sobotková, M., Čejková, B., & Wassenaar, L. I. (2012). Technical Note: Evaluation of between-sample memory effects in the analysis of  $\delta^2\text{H}$  and  $\delta^{18}\text{O}$  of water samples measured by laser spectrometers. *Hydrology and Earth Systems Sciences*, 16, 3925–3933. <https://doi.org/10.5194/hess-16-3925-2012>
- Penna, D., Zanotelli, D., Scandellari, F., Aguzzoni, A., Engel, M., Tagliavini, M., & Comiti, F. (2021). Water uptake of apple trees in the Alps: Where does irrigation water go? *Ecohydrology*, 14(6). <https://doi.org/10.1002/eco.2306>
- Prieto, I., Armas, C., & Pugnaire, F. I. (2012). Water release through plant roots: New insights into its consequences at the plant and ecosystem level. *New Phytologist*, 193(4), 830–841. <https://doi.org/10.1111/j.1469-8137.2011.04039.x>
- Putman, A. L., Fiorella, R. P., Bowen, G. J., & Cai, Z. (2019). A global perspective on local meteoric water lines: Meta-analytic insight into fundamental controls and practical constraints. *Water Resources Research*, 55, 6896–6910. <https://doi.org/10.1029/2019WR025181>
- R Core Team. (2021). R: A language and environment for statistical computing. R Foundation for Statistical Computing. <https://www.R-project.org/>
- Reato, A., Borzi, G., Martínez, O. A., & Carol, E. (2022). Role of rock glaciers and other high-altitude depositional units in the hydrology of the mountain watersheds of the northern Patagonian Andes. *Science of the Total Environment*, 2022, 153968. <https://doi.org/10.1016/j.scitotenv.2022.153968>
- Rempe, D. M., & Dietrich, W. E. (2018). Direct observations of rock moisture, a hidden component of the hydrologic cycle. *Proceedings of the National Academy of Sciences*, 115(11), 2664–2669. <https://doi.org/10.1073/pnas.1800141115>
- Rozanski, K., Araguás-Araguás, L., & Gonfiantini, R. (1993). *Isotopic patterns in modern global precipitation* (Vol. 78). Climate change in continental isotopic records. Geophysical Monograph Series. (pp. 1–36). AGU.
- Schmieder, J., Hanzer, F., Marke, T., Garvelmann, J., Warscher, M., Kunstmann, H., & Strasser, U. (2016). The importance of snowmelt spatiotemporal variability for isotope-based hydrograph separation in a high-elevation catchment. *Hydrology and Earth Systems Sciences*, 20, 5015–5033. <https://doi.org/10.5194/hess-20-5015-2016>
- Somers, L. D., & McKenzie, J. M. (2020). A review of groundwater in high mountain environments. *WIREs Water*, 2020(7), e1475. <https://doi.org/10.1002/wat2.1475>
- Sprenger, M., Leistert, H., Gimbel, K., & Weiler, M. (2016). Illuminating hydrological processes at the soil-vegetation-atmosphere interface with water stable isotopes. *Reviews of Geophysics*, 54, 674–704. <https://doi.org/10.1002/2015RG000515>
- Sprenger, M., Llorens, P., Cayuela, C., Gallart, F., & Latron, J. (2019). Mechanisms of consistently disjunct soil water pools over (pore) space and time. *Hydrology and Earth System Sciences*, 23(6), 2751–2762. <https://doi.org/10.5194/hess-23-2751-2019>
- Sprenger, M., Tetzlaff, D., Buttle, J., Carey, S. K., McNamara, J. P., Laudon, H., Shatilla, N. J., & Soulsby, C. (2018). Storage, mixing, and fluxes of water in the critical zone across northern environments inferred by stable isotopes of soil water. *Hydrological Processes*, 32(12), 1720–1737. <https://doi.org/10.1002/hyp.13135>
- Stock, B. C., Jackson, A. L., Ward, E. J., Parnell, A. C., Phillips, D. L., & Semmens, B. X. (2018). Analyzing mixing systems using a new generation of Bayesian tracer mixing models. *PeerJ*, 6, e5096. <https://doi.org/10.7717/peerj.5096>
- Stock, B. C., & Semmens, B. X. (2016). MixSIAR GUI User Manual. <https://doi.org/10.5281/zenodo.1209993>, Version 3.1, <https://github.com/brianstock/MixSIAR>
- Tetzlaff, D., Buttle, J., Carey, S. K., Kohn, M. J., Laudon, H., McNamara, J. P., Smith, A., Sprenger, M., & Soulsby, C. (2020). Stable isotopes of water reveal differences in plant–Soil water relationships across northern environments. *Hydrological Processes*, 35, e14023. <https://doi.org/10.1002/hyp.14023>
- von Freyberg, J., Allen, S. T., Grossiord, C., & Dawson, T. E. (2020). Plant and root-zone water isotopes are difficult to measure, explain, and predict: Some practical recommendations for determining plant water sources. *Methods in Ecology and Evolution*, 11, 1352–1367. <https://doi.org/10.1111/2041-210X.13461>
- Warren, J. M., Meinzer, F. C., Brooks, J. R., Domec, J.-C., & Coulombe, R. (2007). Hydraulic redistribution of soil water in two old-growth coniferous forests: Quantifying patterns and controls. *New Phytologist*, 173, 753–765. <https://doi.org/10.1111/j.1469-8137.2006.01963.x>
- Wei, L., Qiu, Z., Zhou, G., Zuecco, G., Liu, Y., & Wen, Y. (2022). Soil water hydraulic redistribution in a subtropical monsoon evergreen forest.

- Science of the Total Environment*, 835, 155437. <https://doi.org/10.1016/j.scitotenv.2022.155437>
- Wood, S. (2023). Mixed GAM Computation Vehicle with Automatic Smoothness Estimation. Package *mgcv*, version 1.9–0. <https://cran.r-project.org/web/packages/mgcv/mgcv.pdf>
- Xu, Q., Li, H., Chen, J., Cheng, X., Liu, S., & An, S. (2011). Water use patterns of three species in subalpine forest, Southwest China: The deuterium isotope approach. *Ecohydrology*, 4, 236–244. <https://doi.org/10.1002/eco.179>
- Zhang, Y., Xu, J., Jiang, Y., Mandra, T., Rademacher, T. T., Xue, F., Dong, M., & Pederson, N. (2021). Higher plasticity of water uptake in spruce than larch in an alpine habitat of North-Central China. *Agricultural and Forest Meteorology*, 311, 108696. <https://doi.org/10.1016/j.agrformet.2021.108696>
- Zhu, G., Wang, L., Liu, Y., Bhat, M. A., Qiu, D., Zhao, K., & Ye, L. (2022). Snow-melt water: An important water source for *Picea crassifolia* in Qilian Mountains. *Journal of Hydrology*, 613, 128441. <https://doi.org/10.1007/s10653-022-01472-w>
- Zuecco, G., Amin, A., Frentress, J., Engel, M., Marchina, C., Anfodillo, T., Borgia, M., Carraro, V., Scandellari, F., Tagliavini, M., Zanotelli, D., Comiti, F., & Penna, D. (2022). A comparative study of plant water extraction methods for isotopic analyses: Scholander-type pressure chamber vs. cryogenic vacuum distillation. *Hydrology and Earth Systems Sciences*, 26, 3673–3689. <https://doi.org/10.5194/hess-26-3673-2022>
- Zuecco, G., Carturan, L., de Blasi, F., Seppi, R., Zanoner, T., Penna, D., Borgia, M., Carton, A., & Dalla Fontana, G. (2019). Understanding hydrological processes in glacierized catchments: Evidence and implications of highly variable isotopic and electrical conductivity data. *Hydrological Processes*, 33, 816–832. <https://doi.org/10.1002/hyp.13366>

## SUPPORTING INFORMATION

Additional supporting information can be found online in the Supporting Information section at the end of this article.

**How to cite this article:** Brighenti, S., Obojes, N., Bertoldi, G., Zuecco, G., Censini, M., Cassiani, G., Penna, D., & Comiti, F. (2024). Snowmelt and subsurface heterogeneity control tree water sources in a subalpine forest. *Ecohydrology*, e2695. <https://doi.org/10.1002/eco.2695>